We would like to thank reviewer#1 Rik Wanninkhof for the thoughtful comments and suggestions. In the following we will respond (in italics) to each reviewer comment (printed in bold font) individually

Reviewer Rik Wanninkhof, NOAA/AONL A uniform pCO2 climatology combining open and coastal oceans Peter Landschützer, Goulven G. Laruelle,, Alizee Roobaert, and Pierre Regnier

R#1: The is a nice descriptive paper providing the procedures of merging the coastal pCO2 NN data from Laruelle et al. 2017 with the global fields of Landschützer et al. 2016. It gives an overview of the means of merging, and then provides an extensive analysis of the differences in the region of overlap using several coastal locations as examples. Writing style, syntax and grammar are very good and procedures are clearly described. Figures are of good quality but I wished there would be a way the more clearly show the coastal area that shows up as a thin multi-colored rind in the figures. The paper is an important contribution in documenting the procedures and outcomes of the combining exercise, and shows, on the whole, a consistent final product. Laruelle et al. 2017 mentioned that the products could be "readily merged". As this paper aptly describes the merging is not "readily done" but requires specific procedures, assumption and approaches which are well detailed in this manuscript. My comments below should not be considered a requirement for changing the manuscript, that seems good as is, but rather issues that came to mind while reading the paper. It therefor does not require a point by point rebuttal.

Response: Many thanks for the overall positive assessment of our study and the helpful comments we received. While the reviewer does not ask for a detailed rebuttal, we took this opportunity to provide a point-by-point response describing how we have taken the referee suggestions into account, because we are eager to improve our manuscript and found many of the reviewer's suggestion very useful. We agree with the reviewer that the coastal and overlap bands are somewhat hard to see in Figures 1, 2 and 5 given the global projection we chose (due to the global nature of our study). We have thus tried alternative ways to display the coastal and overlap regions and found that the equidistant projection without longitude/latitude mesh lines offers the best visualization of all coastal features. We have illustrated this below where (a) represents the original version and (b) the new equidistant projection. We therefore adjusted Figures 1, 2 and 5 accordingly.

(a)

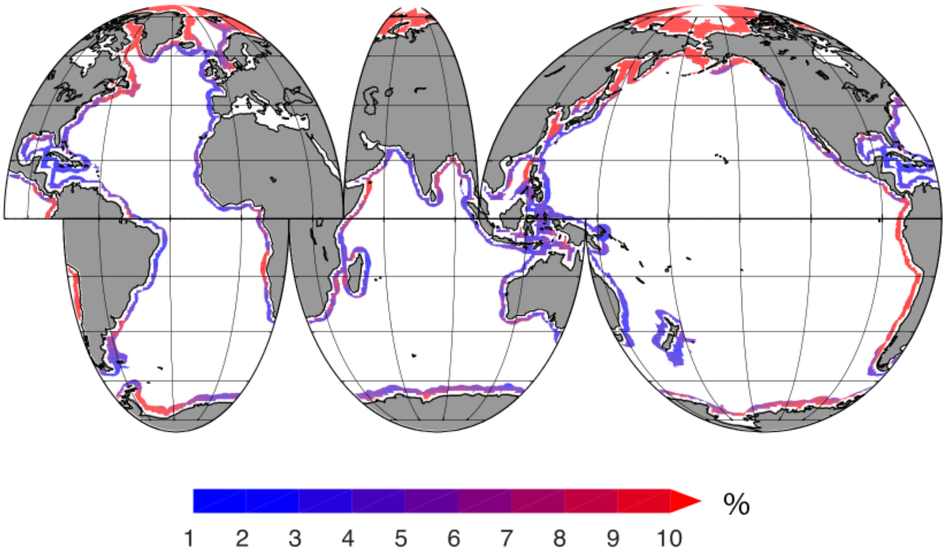

(b)

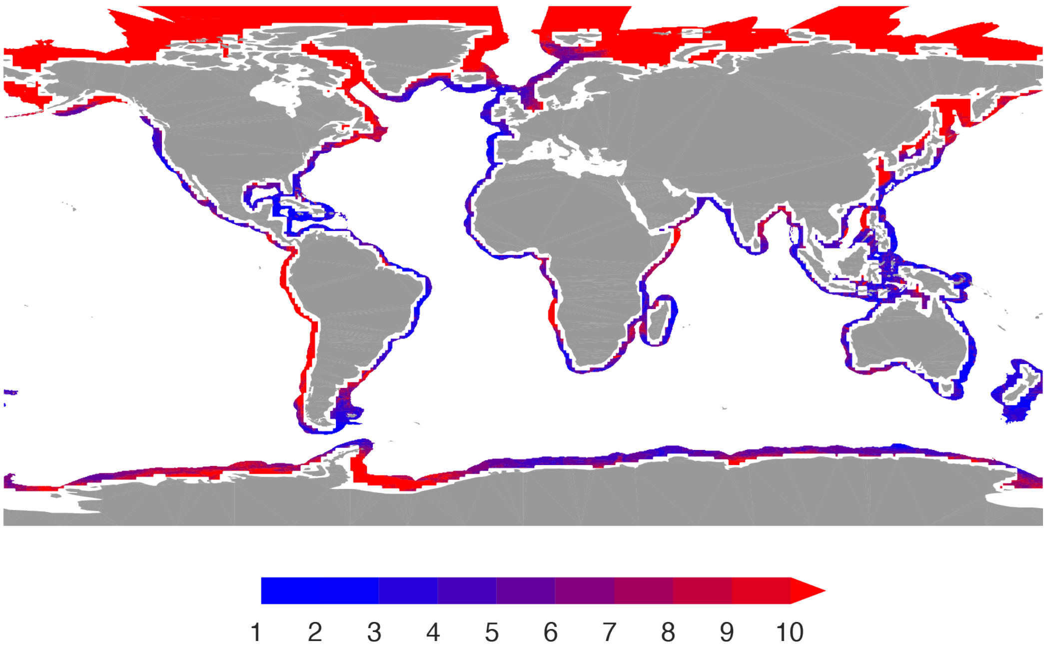

R#1: General comments - There should be some indication of how many observations there really are in the coastal region (and Open ocean overlap). % of pixels with observations (where the pixel is the 0.25 degree monthly "grid box" for the time period) is a good metric for each of the 30 regions investigated.

Response: As both the coastal and open ocean product rely on the gridded SOCAT data, we have now provided this information in the respective methods section, however, unlike suggested by the referee, we have (also as indicated below in response to other comments) refrained from providing a table with the error statistics (bias and standard deviation) and the number of observations for all 30x30 regions since this equates to 72 regions of which 57 are occupied. We believe that this would be a very large and cryptic table with little use to most readers. Hence we thought of alternative ways to display this information and opted for a box-whisker plot which, in our opinion best shows the proposed metrics. We therefore introduce the following new plot (new figure 4 in *the revised manuscript) in our revised manuscript instead of a table that would summarizes the number of data, std and mean difference of coastal ocean and open ocean product for the 30x30 regions*

Additionally, we added the following text to the methods section: "Substantial differences exist between the mean difference and standard deviations of NNopen and NNcoast and the respective measurements from the SOCAT database within each 30x30 degree raster. Figure 4 illustrates these differences. While both NNopen and NNcoast have a near 0 bias for the mean differences, some rasters show differences exceeding 15µatm. While more variability appears in NNcoast, this can largely be explained by to the overall smaller number of gridded measurements. The larger number of gridded measurements in NNopen is a result from the division of the 1x1 degree cells into 16 quarter degree boxes. Therefore, we reduce the number of effective degrees of freedom for the open ocean by 16."

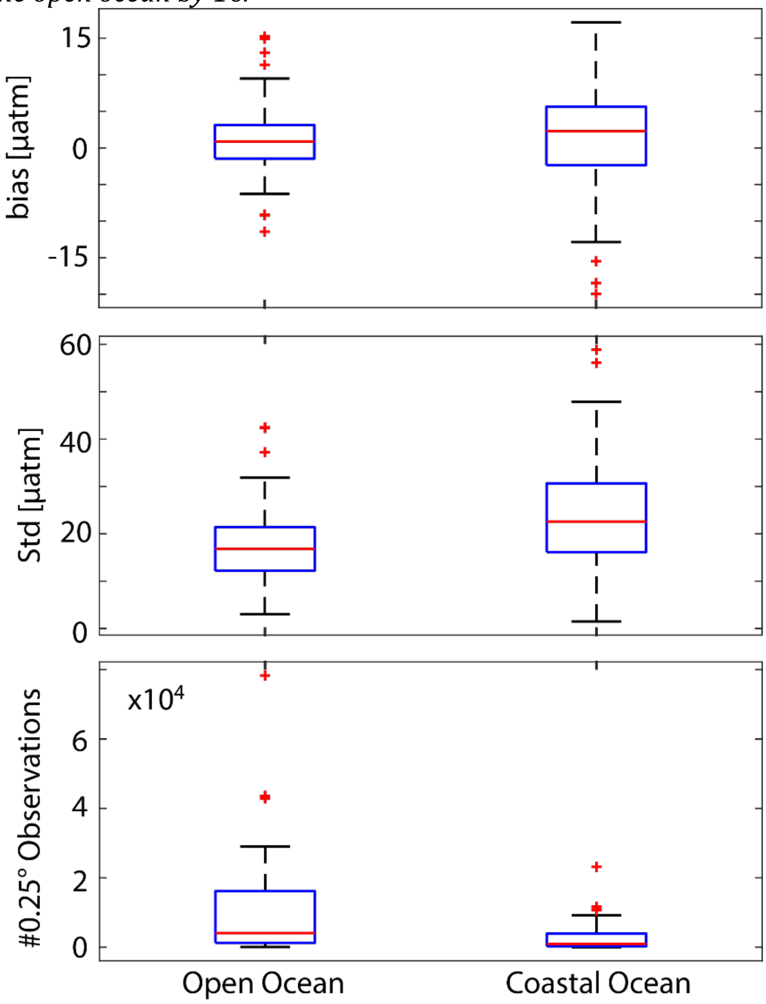

Caption: Box-Whisker plot of the mean difference (top), standard deviation (middle) and number of 0.25° pixels occupied with measurements (bottom) in the common overlap area for each 30°x30° box used for merging NN_{open} and NN_{coast}.

R#1: Different predictors are used for the coastal product and the open ocean dataset. E.g. Coastal uses wind and bathymetry (and sea ice); while the open ocean uses mixed layer depth (MLD). Is there any estimate how different the nn outputs are? That is,

perhaps some mention if the different predictors influence the comparison between open ocean and coastal. In particular, what is the effect of not using MLD in the coastal product when we know large parts of the broad Western shelves are strongly stratified for part of the year?

Response: Besides this study, there is no quantitative assessment of the difference between both products. The reviewer is correct in that the products are different in the use of predictor data. We believe this remark best fits in the conclusions section of the manuscript, hence we have added a paragraph discussion these differences. This paragraph reads:

"Additionally, methodological differences between NNopen and NNcoast, such as differences in predictor data result in local differences, e.g. in ice covered regions where NNcoast relies on sea-ice as predictor or shallow, stratified waters, where mixed layer depth serves as important proxy in NNopen"

R#1: What is not empathized is that in the overlap region the pCO2 observations used in coastal and open ocean products are exactly the same (I believe). - Is the data quality for the coastal data lower than for the open ocean? And, if so, does this have an effect (That is, I believe that that are more SOCAT "C" cruises in the coastal than in the open ocean).

Response: The data in the overlap area are fairly identical, however there is a difference in the resolution of the gridded SOCAT data (which is illustrated in Figures 6 onwards panels b, c, e and f, as well as in the new figure introduced above). Indeed, the resolution of NNopen is 1 degree while the resolution of NNcoast is ¼ degree, which certainly influences the reconstruction. The difference in data quality is an interesting aspect, however we believe such an investigation is beyond the scope of this study, as it would require to check the individual cruises and how they feed into the gridded SOCAT gridded products. Furthermore, we believe that the uncertainty from extrapolating the observations over several hundreds of kilometers in distance contributes more to the overall uncertainty (compared to the 2µatm uncertainty from flag A and B data compared to 5µatm uncertainty from flag C data). Nevertheless, we have mentioned in the text that the gridded SOCAT data comprise of observations that received a flag A-D and therefore a potential uncertainty of 2-5µatm results from the measurement uncertainty.

In particular we added in the methods section: "The gridded SOCAT data consist of measurements that received a quality flag of D and lower, illustrating a measurement uncertainty within 5 µatm."

R#1: Specific comments Page 1. Line 9 "This also illustrates the potential of such analysis to inform the measurement community about the locations where additional measurements are essential to better represent the aquatic continuum": This is also mentioned in the conclusions but I do not see clear evidence of how this is the case.

We have rephrased this statement on page 1 to: "This also illustrates the potential of such analysis to highlight where we lack a good representation of the aquatic continuum and future research should be dedicated."

Regarding the sentence in the conclusion section, we expanded upon this statement to provide explicit recommendations based on the findings of this manuscript. In particular, we mentioned the Peru upwelling system and the high latitude regions, since we face a critical monthly difference between open ocean and coastal ocean reconstructions (see Figures 5 and 13), and we believe that this huge gap cannot be closed by improving the methods, but only by observing the field pCO2.

We therefore added: "The overlap analysis proposed here and particularly the Percent mismatch and RMSE analysis, further serves as a benchmark on how well we understand the coastal-to-open *ocean continuum and its spatial variability and where we still lack essential measurements to close the gap between existing estimates, such as e.g. the Peruvian upweling system or the seasonally ice-covered high latitude regions, in particular the Arctic Ocean"*

R#:1Page 3. Line 5 "whereas Roobaert et al. (2019) suggests that this difference stems from the uneven latitudinal distribution of surface areas between coastal and open ocean but that adjacent open and coastal regions behave similarly.": I don't understand this.

Response: We rephrased this to: "… whereas Roobaert et al. (2019) suggests that adjacent open and coastal regions behave similarly."

R#1: Page 3, line 15. "As a significant fraction of this CO2 outgassing derived from terrestrial carbon inputs likely takes place near the coast or across the coastal-open ocean transition,": I believe that the working assumption is that this outgassing occurs in the southern hemisphere far away from the rivers (due to slow oxidation of riverine supplied terres- trial organic matter).

Response: Only a small amount of the riverine derived CO2 outgases in the Southern Ocean (compared to the large outgassing of natural carbon resulting from the upwelling of old carbon rich waters - see e.g. Figure 1b in Gruber et al 2009, "Oceanic sources, sinks, and transport of atmospheric CO2", Global Biogeochemical Cycles). The largest river outgassing fluxes – according to the work of Gruber et al 2009 and Mikaloff-Fletcher et al 2007 (Inverse estimates of the oceanic sources and sinks of natural CO2 and the implied oceanic carbon transport, Global Biogeochemical Cycles, 21, GB1010.) take place in the Northern hemisphere where most river input are delivered into the coastal ocean. This statement further refers to the work of Regnier et al 2013 (Figure 1a in "Anthropogenic perturbation of the carbon fluxes from land to ocean", Nature Geosciences) who do show that the Land Ocean Aquatic Continuum plays a significant role in redistributing carbon from riverine input. No changes have been made in the manuscript.

R#1: Page 4: It would be illustrative to show a map of the different provinces for coastal and open ocean (I know the boundary are not fixed but they do not vary that much)

Response: Many thanks for this suggestion. These province maps however are already introduced in Landschützer et al 2014 and Laruelle et al 2017. We have now mentioned in the text that these province maps can be found in these respective manuscripts.

In particular we added to the second paragraph in the methods section: "These provinces are illustrated in Landschützer et al 2014 and Laruelle et al 2017"

R#1: Page 4 line 20 "Firstly, we replaced the mixed layer depth proxy of the NNopen from de Boyer Montegut et al. (2004) to the Argo based MIMOC product": a. How much difference does this make?; and b. If it is purely ARGO based it will be for water depths > 1200 m so much of the open ocean coastal overlap would not have good MLD.

Response: a) we noted in the text, lines 21-22: "while the error statistics of the method remain nearly unchanged". We understand however, that this is fairly vague, hence we expanded a little further and wrote: "We tested the impact of this change and found that SOCAT observations are reconstructed bias free with a root mean squared error of less than 20µatm similar to Landschützer et al 2016"

b) This was a mistake on our end: The MIMOC MLD product is not entirely ARGO based, but combines (quoting from Schmidtko et al 2012): "All available quality- controlled profiles of temperature (T) and salinity (S) versus pressure (P) collected by conductivity-temperature-depth

(CTD) instruments from the Argo Program, Ice-Tethered Profilers, and archived in the World Ocean Database are used". We have corrected this in the text. For a detailed view of the profiles used and a comparison to other products such as de Boyer Montegut et al 2004, we can refer the referee to the original publication about the MIMOC mixed layer depth product: Schmidtko, S., G. C. Johnson and J. M. Lyman, 2013. MIMOC: A Global Monthly Isopycnal Upper-Ocean Climatology with Mixed Layers. Journal of Geophysical Research, 118, in press, doi: 10.1002/jgrc.20122.

We have now removed "Argo based" from the text.

R#1: Page 7. Line 14 "N is the number of available gridded data from SOCATv5 available in a given 30x30 raster box and the subscript I refers to either NNopen or NNcoast": This information would be of interest as a table for each 30 by 30 region

Response: We understand the interest in such a table, however, given that there are 12x6 such raster boxes (although not all are covered by both products), this table would be huge and would provide little information compared to its dimension. We therefore decided to introduce the error metric figure above to inform the reader (see comment 2 above). The number of 0.25° measurements is displayed in the lower panel.

R#1: Page 8. Line 17 "Figure 5 reports the absolute pCO2 difference in % between NNcoast and NNopen along the common overlap area relative to the mean partial pressure of the merged climatology.": Including this in a table for each province or 30 by 30 region along with the st deviation would be illustrative. Table 1- providing the % of coastal-no obs. And % coastal-open collocated would be of interest.

Response: We have included these error metrics for each 30x30 region in a new figure (see comment 2 above). We have, however decided to use absolute differences towards the actual measurements and std instead of % error in this case as open ocean and coast may be better comparable this way and since these are the metrics used for the merging. We further believe that figure 5 (now figure 6 in the revised manuscript) clearly illustrates the mismatch in % more refined in space (i.e. for each 0.25° grid box)

R#1: Fig 6. Providing the standard deviation of the mismatch shown d,e,f as extra panels would be of interest.

Response: Displaying the standard deviation of the mismatch in time as additional panel in the map is problematic for 2 reasons. Firstly, we believe that the spatially refined std is not always very meaningful for all chosen regions (with the exception of data rich regions, e.g. of the US coast, where repeat occupations exist) since very few ¼ degree pixels are occupied more than once in time. This is illustrated by the Amazon river outflow region below (color axis in µatm). Secondly, our figures already consist of 6 panels and we are afraid to "overload" the manuscript with figures that way. Instead we provide the RMSE in table 2 of the original manuscript for each region as we believe this provides an equally meaningful metric for the entire region.

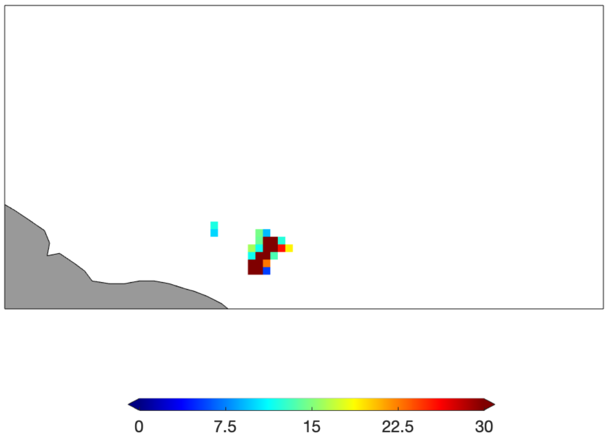

Caption: Standard deviation of the mismatch as illustrated for the coastal ocean observations within the Amazon outflow region.

R#1: Fig 7- 12 repeating the legend rather than stating "like Fig 6" will make reading the paper a bit easier

Response: we have now repeated the legend for all figures.

R#1: Page 13. Line 5 "The area is spatially well covered both in the open and coastal ocean SOCAT datasets": It would be worthwhile to quantify what "well covered means" .

Response: We agree that the term "well covered" was not clear. In this particular case we rephrased to "... spatially covered both in the open and coastal ..."

R#1: Page 15. "Some of the best monitored regions spanning both coastal and near-shore open ocean can be found along the US coast (Fennel et al., 2008; Laruelle et al., 2015; Fennel et al., 2019)": Perhaps include refer- ence to "Signorini, S. R., Mannino, A., Najjar, R. G., M., F. M. A., Cai, W.-J., Salisbury, J., Wang, Z. A., Thomas, H., and Shadwick, E. H.: Surface ocean pCO2 seasonality and sea-air CO2 flux estimates for the North American east coast, J. Geophys. Res., 118, doi:10.1002/jgrc.20369, 2013."

´*Response: We have now added the additional reference in the revised manuscript*

R#1: Page 15: "climatological nature of the merged product, which does not reflect the variable upwelling as a result of interannual variability linked to ENSO events.": Could this be verified by looking at the standard deviation?

Response: We believe that this would require more research than looking at the Standard deviation and is beyond the scope of this study. Nevertheless, we also note that the formulation was not entirely clear. Hence we rephrased our sentence into: "The small error compared to the SOCAT observations suggests that this is not the result of the 2 products being in disagreement but might relate to changes in upwelling as a result of interannual variability linked to ENSO events that are not well captured by the merged product."

R#1: Page 17. Figure 10 The N- S spatial trend in panels d-f is pretty apparent. While it is alluded to in the text the description seems a bit vague.

Response: We have now added extra emphasis to this difference

We added "Landschützer et al. (2014) attributed a larger mismatch to the complex biogeochemical dynamics of the Gulf Stream region, where the measured pCO2 is underestimated by both the open and coastal products. The strong mesoscale dynamics and the influence of the cold Labrador current in this region are not well represented in the rather coarse 0.25° NNcoast and 1° NNopen products"

We would like to thank reviewer#2 for the thoughtful comments and suggestions. In the following we will respond (in italics) to each reviewer comment (printed in bold font) individually

R#2: The reviewer enjoyed this article very much because the authors described how they merged open and coastal ocean pCO2 mapped climatology. The reviewer also observed that writing nature is very clear and good and procedures that they did are very clearly described. It is however the reviewer would like to suggest some to improve this article, therefore this article can be published ESSD after minor revision as stated below.

Response: Many thanks for the positive evaluation of our manuscript

R#2: 1, Page 4 line 4- On the data treatment about the overlapping area: The authors defined the open region and the coastal region as "covering broadly the open ocean at a distance of 1°, off the coast and, the second dataset, by Laruelle et al. (2017), covering the coastal domain plus the adjacent open ocean up until 400km away from the shoreline". And in page 6 line 2 the authors stated "landward limit of the NNopen is located on average at around 1° (or roughly 100km) offshore". As the authors know 1 degree latitude is almost 110.6 km to 111.7 km but 1 degree longitude depends on latitude and varied from 111.2 km to zero. Therefore the authors should make clear how they define and treat the data as the open ocean.

Response: We concur that using ° and km interchangeably without further explanation may cause confusion. The open ocean product is defined as the ocean area 1° away from shore, which is – as stated by the referee depending on geographical position – variable in km. The Laruelle estimate on the other hand uses the 400km definition, i.e. it is not variable depending on latitude. We have clarified this in the text at the positions indicated by the referee.

In particular, on page 6 lin2 we added: "While the landward limit of the NNopen is located at 1° (and therefore varies in km depending on the geographical position) off shore, …"

In the conclusions section we further added: " … leading to an overlap domain of roughly 300km close to the equator and increasing in extend towards the poles around the land surface"

R#2: 2, page 7. Figure 3 is important to understand how the authors merged the open ocean product and the coastal region product. Therefore it might better to enlarge this figure 3. The reviewer also suggests adding a numerical table to show an example of how they merged.

Response: We have now rearranged figure 3 so it appears larger in the manuscript (see figure (a) below). Additionally, we have added another figure (instead of a table – see (b) below) highlighting the statistics of the merging algorithm (new figure illustrated below including number of observations, mean differences and std differences within each 30x30 box). We believe that the newly introduced box-whisker plot is easier to grasp than an example highlighted in a numeric table.

(a)

(b)

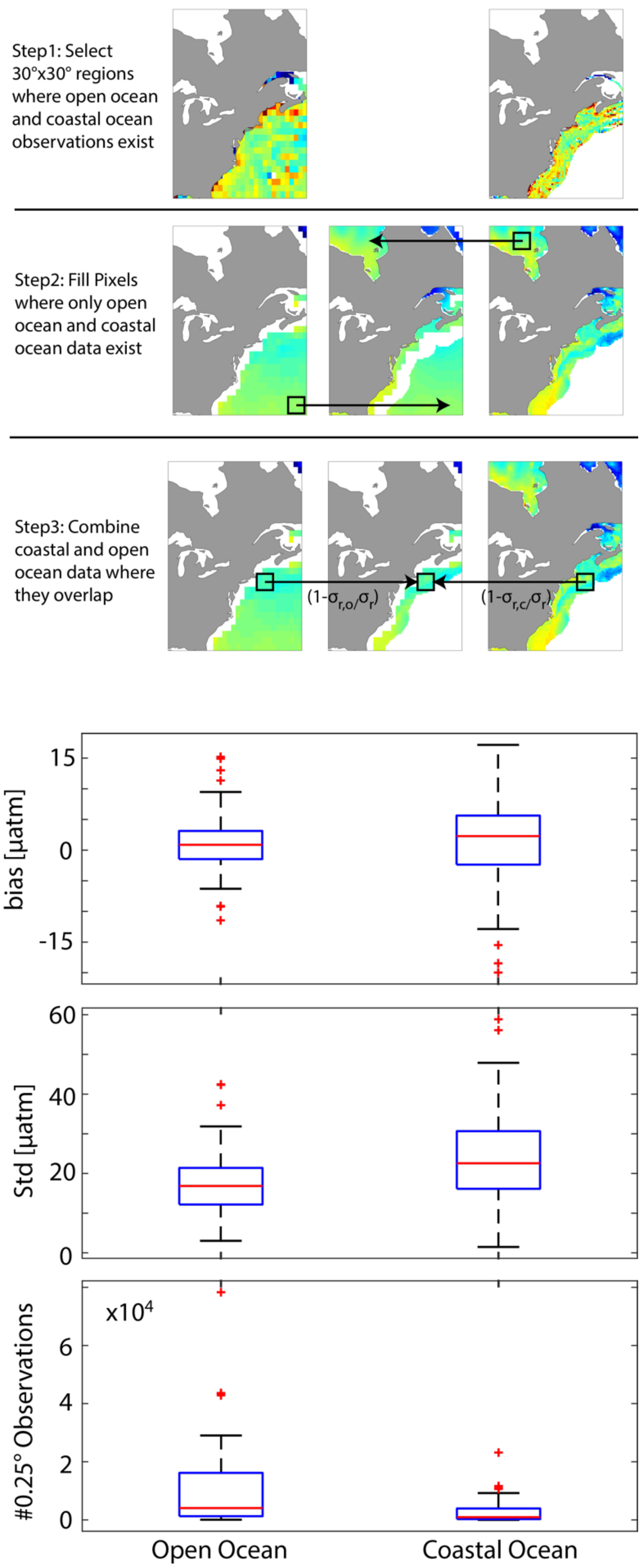

Step1: Select 30°x30° regions where open ocean and coastal ocean observations exist
Step2: Fill Pixels where only open ocean and coastal ocean data exist
Step3: Combine coastal and open ocean data where they overlap
(1-σr,o/σr)
(1-σr,c/σr)
bias [µatm]
15
0
-15
Std [µatm]
60
40
20
0
#0.25° Observations
x10^4
6
4
2
0
Open Ocean
Coastal Ocean

R#2: 3, page 10 In the Figure 5, the maximum of a color bar of mismatch percent means that clear red indicates exceed 10 %. The reviewer suggests extending this color bar at least 15 % or 20 % to clearly show the regions where the mismatch is large because a smaller mismatch region does not need to highlight but a larger mismatch region should be highlighted.

Response: We have now increased the maximum value of the colorbar accordingly to 15% and changed the color palette to better highlight regions with larger mismatch (see updated figure below). We concur that we could further expand the upper limit, however, we would therefore miss to represent the geographical finer scale differences (e.g. along the Antarctic continent).

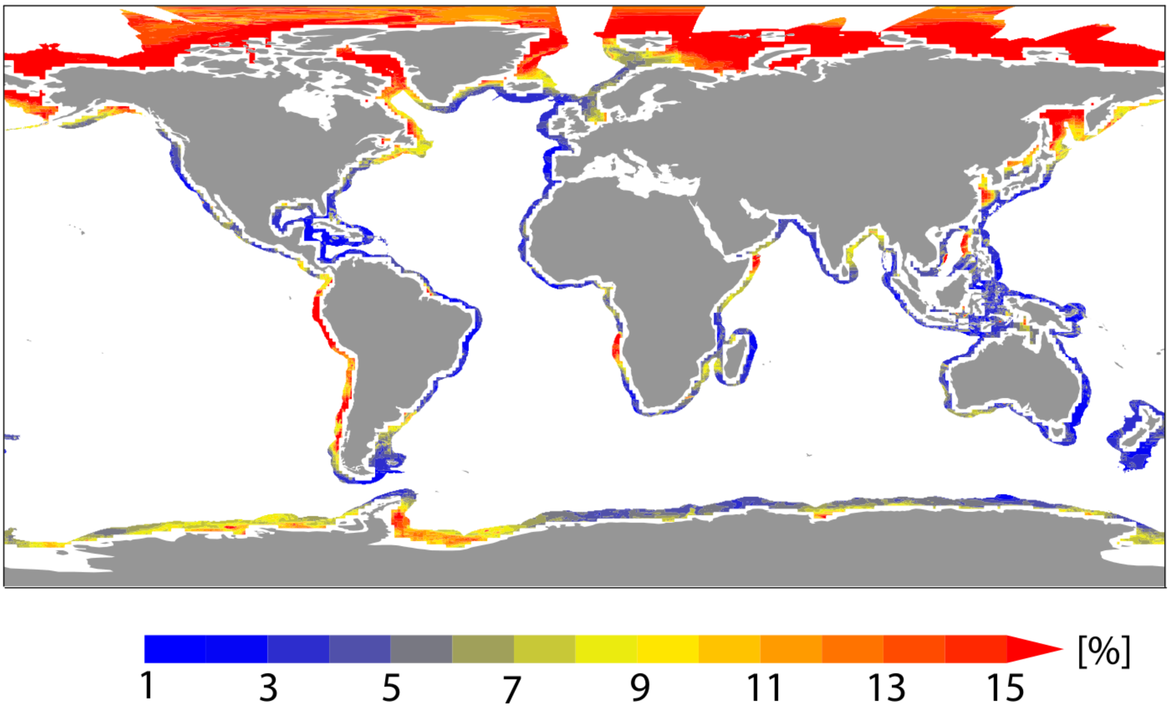

R#2: 4, Page 14 line 3. The authors discussed about Sea of Japan. It is however this region is a marginal sea and it not appropriate to compare NNopen and NNcoast here because the Sea of Japan might be included into coastal region following 400 km definition from the Japanese coast and Korean/Russian coast. Furthermore, there are probably no observed data at the Korean/Russian side based on Figure 9 (c). Therefore it is better to delete this part from this article.

Response: Many thanks for this keen observation. As can been seen in Figure 2 and Figure 9 of the manuscript, both open ocean and coastal ocean datasets in the SOCAT databases include measurements from the Sea of Japan. That said, we believe that including a marginal Sea in this intercomparison is an exciting opportunity to compare how both open ocean and coastal ocean reconstructions are able to represent in a marginal sea. We see this as relevant information to users who want to use the product to investigate this and other marginal seas. As illustrated in Figure 9 e and f, both products struggle to reproduce the available data, which indeed may be related to the fact that coastal and open ocean products have difficulties reconstructing the dynamics of this marginal Sea. So instead of removing this part, we have expanded the discussion of the mismatch in light of the fact that this region comprises a marginal sea.

In particular, we added in the first paragraph of the Regional Analysis section: ", two data rich regions (Sea of Japan, US east coast) of which one comprises a marginal sea (Sea of Japan), one *region where seasonal data are scarce (West Coast of Australia), and a region characterized by strong river outflow (Amazon river plume)."*

We also extended the discussion regarding the Sea of Japan which now reads: "The strong variability in the observed pCO2 reflects the complex carbon dynamics in the Sea of Japan (Chen et al 1995, Park et al 2006), which is also reflected in the larger mismatch between products and towards the SOCAT observations (figures 10 d-f). The disagreement may indicate that the global scale NNopen and NNcoast products are not particularly skilled in representing the strong regional dynamics of marginal sea."

Finally, we added to the conclusions: "However, stronger differences exist in other parts of the world, particularly in the Peruvian upwelling system, the Arctic and Antarctic, the African coastline in the South Atlantic and the Arabian Sea, where fewer observations exist. Additionally, we find larger discrepancies in the marginal Sea of Japan."

R#2: 5, Figure 6,7,8,9,10,11,12: In (d)(e)(f) of these 7 figures, it is a little bit difficult to see the differences. Especially to distinguish difference zero region and no data region because the authors assigned no fill to both regions. Please re-draw these figures.

Response: We concur that differences close to 0 are more difficult to spot, and we have therefore adjusted the colorbar accordingly so that 0 values are not displayed white. We nevertheless chose a "soft color", i.e. yellow, to display values close to 0 as we intend to highlight discrepancies from 0 in these plots. Below is an example of the reworked figures (using the Amazon outflow as example region)

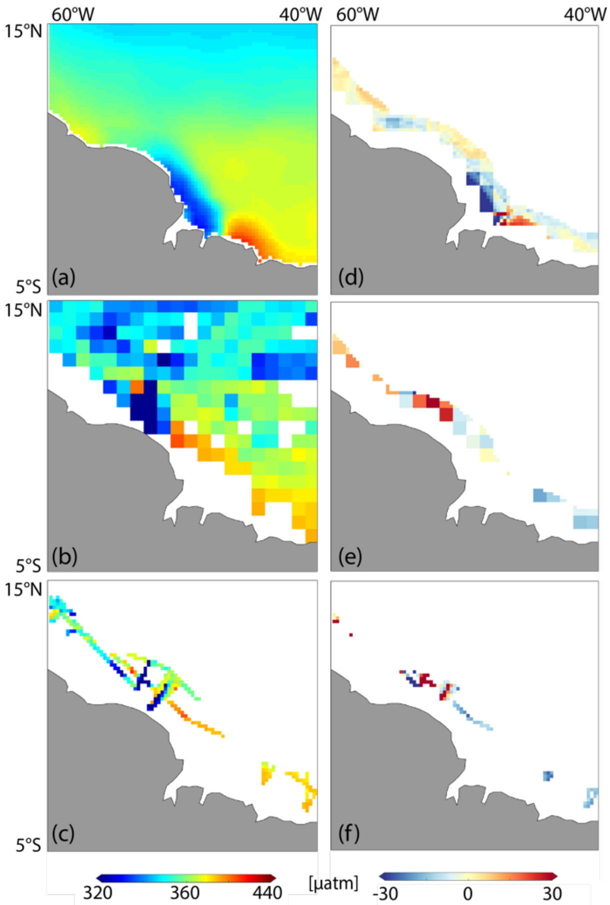

R#2: 6, P21 line 19- The authors stated that "Despite the lack of seasonal observations along the West coast of Australia, both products agree well with regards to the seasonal cycle and differences stay within of 8-10µatm between the different products.". The reviewer observed in figure 13 that in these three regions NNopen and NNcosat products showed a minimum or a maximum although there are no observed data at the time of a minimum or a maximum, eg. a minimum in September on the west coast of Australia. The reviewer cannot understand how NNopen and NNcosat products there were produced and showed a minimum/maximum. Please explain this.

Response: Both products (coast and open ocean) are the result of a neural network interpolation of all available observations regressed onto driver data (see also methods here and in Landschützer et al 2014 and Laruelle et al 2017 cited in this work). Whenever there are no local observations available, the pCO2 is reconstructed from observations that fall within the same biogeochemical province, defined by a self-organizing map algorithm. In a second step all observations from the same province are regressed against physical (temperature, salinity, mixed layer depth), chemical (atmospheric CO2) and biological (chlorophyll a) driver data using a non-linear neural network-based regression approach (a feed-forward network). Based on the variability of these driver data the resulting pCO2 fields show variability in space and time and – in this particular case – a minimum in September largely owing (as we believe) to the solubility pump.

R#2: 7, Page 21 line 17- The authors stated that "Therefore, the combined pCO2 climatology is not only a step forward in including the full oceanic domain with all its complexity into carbon budget analyses, but also help identify areas where additional continuous observations are critically needed to close current knowledge gaps.". The reviewer completely agree this statement and would like to suggest to add some recommendations explicitly from the authors to the community about areas where additional continuous observations are critically needed to close current knowledge gaps. If the authors do so, the contribution of this article to the community will increase much.

Response: We now expanded on this statement to provide explicit recommendations based on the findings of this manuscript. In particular, we mentioned the Peru upwelling system and high latitudes as prime example, since we face a critical monthly difference between open ocean and coastal ocean reconstructions, and we believe that this huge gap cannot be closed improving the methods, but only by observing the true pCO2.

In particular, we added to the conclusions: "The overlap analysis proposed here and particularly the Percent mismatch and RMSE analysis, further serves as a benchmark on how well we understand the coastal-to-open ocean continuum and its spatial variability and where we still lack essential measurements to close the gap between existing estimates, such as e.g. the Peruvian upwelling system or the seasonally ice-covered high latitude regions, in particular the Arctic Ocean"

A uniform pCO_2 climatology combining open and coastal oceans

Peter Landschützer[1], Goulven G. Laruelle[2,], Alizee Roobaert[2], and Pierre Regnier[2]

[1]Max Planck Institute for Meteorology, Hamburg, Germany

[2]Department Geoscience, Environment & Society (DGES), Université Libre de Bruxelles, Brussels, CP16002, Belgium

Correspondence to: Peter Landschützer (peter.landschuetzer@mpimet.mpg.de)

Abstract.

In this study, we present the first combined open and coastal ocean pCO_2 mapped monthly climatology (Landschützer et al. (2020), doi: 10.25921/qb25-f418, https://www.nodc.noaa.gov/ocads/oceans/MPI-ULB-SOM_FFN_clim.html) constructed from observations collected between 1998 and 2015 extracted from the Surface Ocean CO_2 Atlas (SOCAT) database. We combine two neural network-based pCO_2 products, one from the open ocean and the other from the coastal ocean, and investigate their consistency along their common overlap areas. While the difference between open and coastal ocean estimates along the overlap area increases with latitude, it remains close to 0 μatm globally. Stronger discrepancies, however, exist on the regional level resulting in differences that exceed 10% of the climatological mean pCO_2, or an order of magnitude larger than the uncertainty from state of the art measurements. This also illustrates the potential of such analysis to ~~inform the measurement community about the locations where additional measurements are essential to better represent~~ highlight where we lack a good representation of the aquatic continuum and ~~improve our understanding of the carbon exchange at the air water interface~~future research should be dedicated. A regional analysis further shows that the seasonal carbon dynamics at the coast-open interface are well represented in our climatology. While our combined product is only a first step towards a true representation of both the open ocean and the coastal ocean air-sea CO_2 flux in marine carbon budgets, we show it is a feasible task and the present data product already constitutes a valuable tool to investigate and quantify the dynamics of the air-sea CO_2 exchange consistently for oceanic regions regardless of its distance to the coast.

1 Introduction

Since the beginning of the industrial revolution, human activities such as fossils fuel energy combustion, cement production and land used change have emitted a large quantity of carbon dioxide (CO_2) in the atmosphere disturbing the global carbon cycle and inducing global climate change (Friedlingstein et al., 2019). The ocean plays a fundamental role in understanding the fate of anthropogenic carbon dioxide since it acts as a CO_2 sink and removes roughly 25 % of the anthropogenic CO_2 emitted into the atmosphere every year (Friedlingstein et al., 2019). However, uncertainties are still associated to this estimate, especially in highly heterogeneous and/or poorly monitored regions such as the Arctic Ocean, the southeast Pacific and the coastal ocean

(Regnier et al., 2013; Laruelle et al., 2014). Reducing the uncertainty of current marine CO_2 sink estimates is however essential to improve our understanding of the underlying processes controlling the contemporary and future distribution of anthropogenic CO_2 between atmosphere, land and ocean.

While current oceanic CO_2 sink estimates largely rely on the output from hindcast simulations of global biogeochemistry models (Sarmiento et al., 2010; Le Quéré et al., 2018) and atmospheric as well as oceanic inverse models (Mikaloff Fletcher et al., 2006; Gruber et al., 2009; Wanninkhof et al., 2013), several observation-based estimates built on surface ocean CO_2 measurements emerged in the past years (Landschützer et al., 2014; Rödenbeck et al., 2015; Zscheischler et al., 2017; Laruelle et al., 2017). These estimates are, in part, the result of the community effort that led to the establishment of two large and still growing collections of surface ocean CO_2 measurements, namely the LDEO database (Takahashi et al., 2018) and the Surface Ocean CO_2 Atlas (SOCAT) database (Pfeil et al., 2013; Sabine et al., 2013; Bakker et al., 2014, 2016).

The oceanic uptake of CO_2 is directly proportional to the partial pressure difference of CO_2 ($\Delta p CO_2$) between the oceanic surface water and the atmosphere. Therefore, the increase in available observations from roughly 6 million in the first release of the SOCAT database (SOCATv1.5) in 2011 (Pfeil et al., 2013) to a total of more than 23 million observations gathered in version 6 (SOCATv6) (Bakker et al., 2016), resulted in increasingly detailed and accurate observational-based studies investigating the ocean carbon sink (Rödenbeck et al., 2015). While earlier work such as Takahashi et al. (2009) focused on the long term mean CO_2 uptake and its spatial and seasonal variations, the sustained increase in data density now allows investigating temporal variations on longer time scales (Rödenbeck et al., 2014; Majkut et al., 2014; Landschützer et al., 2014; Rödenbeck et al., 2015; Jones et al., 2015; Landschützer et al., 2016), suggesting a variable ocean CO_2 sink on interannual to decadal timescales (Rödenbeck et al., 2015; Landschützer et al., 2015). These estimates, however, suffer from two main sources of uncertainty. The first related to the kinematic transfer of CO_2 across the air-sea interface (Wanninkhof and Trinanes, 2017; Roobaert et al., 2018) and a second, less well quantified, source related to the interpolation of sparse surface ocean partial pressure of CO_2 data (e.g. Rödenbeck et al., 2015; Landschützer et al., 2014).

Similar to the open ocean, coastal regions - defined here following the broad SOCAT boundary definition of 400km distance from shore used in Laruelle et al. (2017) - are also recognized as a CO_2 sink for the atmosphere (e.g. Laruelle et al., 2014) but have long been constrained using scarce data of uneven spatial and temporal distribution (Thomas et al., 2004; Borges et al., 2005; Cai et al., 2006; Chen and Borges, 2009; Laruelle et al., 2010; Cai, 2011; Chen et al., 2013; Dai et al., 2013). Therefore, because of the strong physical and biogeochemical heterogeneity of the coastal ocean, a proper representation of the spatio-temporal patterns in CO_2 fluxes could only be achieved in the best-monitored regions of the world (Laruelle et al., 2014). More recently, the application of neuronal network-based interpolation methods similar to those applied for the open ocean resulted in the first continuous global $p CO_2$ climatology for the coastal ocean, which improved the estimation of coastal carbon sink and its spatial variability (Laruelle et al., 2017; Roobaert et al., 2019). It is also only very recently that studies have performed a global-scale analysis of the seasonal variability of the air-water CO_2 exchange (Roobaert et al., 2019).

As an additional challenge, many different boundaries have been used to delineate the frontier between coastal and open ocean waters in the past (Walsh, 1988; Borges et al., 2005; Liu et al., 2010; Laruelle et al., 2010, 2013). The choice of a specific delineation has nevertheless important implications for the quantification of the coastal CO_2 sink as well as the adjacent open ocean sink and their temporal trends (Laruelle et al., 2014, 2018). Including the contribution of the coastal ocean in observation-based air-sea CO_2 exchange estimates, i.e. the aim of this study, is not only important in order to improve the quantification of the present-day global ocean sink which has so far been based on open ocean data only, but also to properly analyse the trends and spatio-temporal variabilities of all ocean waters in a consistent manner. Several recent studies have indeed suggested that, as a whole, the intensity of the CO_2 sink per unit area could be stronger in coastal regions than in the open ocean (Borges et al., 2005; Cai, 2011; Laruelle et al., 2010, 2014), whereas Roobaert et al. (2019) suggests that ~~this difference stems from the uneven latitudinal distribution of surface areas between coastal and open ocean but that~~ adjacent open and coastal regions behave similarly.

This distinct behavior of the coastal ocean, with possibly a stronger present-day uptake and a fast-increasing air-sea $p\mathrm{CO_2}$ gradient on decadal timescales is not only relevant for today's quantification of the ocean sink, but also for constraining the anthropogenic perturbation of the marine CO_2 sink. So far, the latter has only been estimated by assuming similar changes in open ocean and coastal seas CO_2 flux densities since pre-industrial times (Wanninkhof et al., 2013; Regnier et al., 2013) while other studies have proposed larger anthropogenic perturbations for the shallow parts of the ocean by mostly relying on conceptual modeling approaches (e.g. Bauer et al., 2013). The need for a unified coastal-open ocean $p\mathrm{CO_2}$ climatology is further reinforced by the recent upward revision of the pre-industrial global ocean CO_2 outgassing fuelled by the river carbon loop (Kwon et al., 2014; Resplandy et al., 2018). As a significant fraction of this CO_2 outgassing derived from terrestrial carbon inputs likely takes place near the coast or across the coastal-open ocean transition, it is important to establish a global ocean $p\mathrm{CO_2}$ climatology that can be used as benchmark for increasingly refined models reconstructing the historical evolution of the marine carbon sink.

As a first step towards this goal, we combine two state-of-the-art sea surface observational $p\mathrm{CO_2}$ products for the open ocean and the coastal regions to create a common global $p\mathrm{CO_2}$ climatology that covers the entirety of the global ocean to better represent the spatio-temporal patterns in the overall marine carbon sink. The combined data product is the first continuous coastal-open ocean $p\mathrm{CO_2}$ climatology constructed with a near-uniformly treated dataset. It also includes the Arctic Ocean, which was not considered in previous open ocean global analyses (Landschützer et al., 2014; Landschützer et al., 2016) and was only partly included in the coastal $p\mathrm{CO_2}$ climatology of Laruelle et al. (2017). In spite of its relatively limited surface area and a significant proportion of seasonal sea ice coverage which prevents most of the gas exchange (Lovely et al., 2015), the Arctic Ocean and its extensive continental shelves is a major contributor of the global coastal CO_2 sink (Yasunaka et al., 2016), displaying some of the most intense air-water CO_2 exchange rate per unit area (Roobaert et al., 2019). The incorporation of these high-latitude regions is thus essential to avoid a bias when analyzing the role of the coastal zone on the global ocean CO_2 sink.

Here, using the new global ocean $p\mathrm{CO_2}$ climatology as well as the individual coastal and open ocean data products, we investigate how well the coastal-open ocean continuum is reconstructed through statistical error analysis. In particular, our goal is to address the following research questions: 1) to what extent reconstructed $p\mathrm{CO_2}$ estimates from both products agree with one another in regions where they overlap; 2) to what extent eventual mismatches are related to data sparsity, both for the temporal $p\mathrm{CO_2}$ mean and the seasonal climatology.

2 Methods

2.1 Open ocean and coastal datasets

Our analysis is based on two recently published sea surface $p\mathrm{CO}_2$ data products. The first one, updated from Landschützer et al. (2016), covering broadly the open ocean at a distance of 1° off the coast and, the second dataset, by Laruelle et al. (2017), covering the coastal domain plus the adjacent open ocean up until 400km away from the shoreline for a total surface area of 70x10^6 km2. Both datasets are based on the same neural network interpolation method, i.e. the SOM-FFN (Self Organizing Map - Feed Forward Neural Network) method (Landschützer et al., 2013). While the individual datasets (from here onward "NN_{open}" for the open ocean dataset and "NN_{coast}" for the coastal ocean dataset) have been extensively described and validated in their individual publications Landschützer et al. (2014); Landschützer et al. (2016); Laruelle et al. (2017), we present here a short summary of each product including their most recent updates and the procedure used to merge both datasets.

The SOM-FFN method consists of a 2-steps interpolation approach. First, a marine region (i.e. either open ocean or coastal ocean) is divided into biogeochemical provinces based on similarities within selected environmental CO_2 driver data. These provinces are illustrated in (Landschützer et al., 2014) and (Laruelle et al., 2017). Secondly, the non-linear relationship between a second set of driver data and available sea surface $p\mathrm{CO}_2$ data from the gridded SOCAT database is established and can then be used to fill gaps where no observations exist (see Landschützer et al., 2013). The gridded SOCAT data consist of measurements that received a quality flag of D and lower, illustrating a measurement uncertainty within 5μatm. Both open and coastal ocean applications rely on satellite and reanalysis data, but different sets of environmental driver variables are used. For the open ocean analysis, sea surface temperature, salinity, mixed layer depth, chlorophyll-a and atmospheric CO_2 are used as proxy variables.

While leaving NN_{coast} unchanged to its original publication (Laruelle et al., 2017), we here provide two updates to NN_{open} compared to its previous publications (see Landschützer et al., 2013, 2014). Firstly, we replaced the mixed layer depth proxy of the NN_{open} from de Boyer Montegut et al. (2004) to the ~~Argo based~~ MIMOC product (Schmidtko et al., 2013) as it allows us to expand our analysis region, creating a maximum overlap area between NN_{open} with NN_{coast}~~, while the error statistics of the method remain nearly unchanged~~. We tested the impact of this change and found that SOCAT observations are reconstructed bias free with a root mean squared error of less than 20 μatm similar to Landschützer et al. (2016). Secondly, for completeness, we also include the Arctic Ocean in NN_{open}, allowing the comparison between products to be extended to the high latitudes. In order to achieve this, the Arctic Ocean was assigned its own stand-alone oceanic biome in the SOM procedure (see Landschützer et al., 2013). Previous global-scale studies avoided the Arctic Ocean (Takahashi et al., 2009; Landschützer et al., 2014), however more recent studies by Yasunaka et al. (2016) illustrate that the increase in measurements makes a reconstruction feasible. Due to its uniqueness in its seawater properties, we find that assigning the Arctic Ocean a stand-alone biome, which is not varying in time, provides the best reconstruction. This way, the Arctic $p\mathrm{CO}_2$ is only determined by Arctic Ocean measurements (starting at 79N in the Atlantic Ocean) while Arctic Ocean measurements are not influencing other biomes. Hence, the remainder of the global ocean remains unchanged by this addition and the $p\mathrm{CO}_2$ product is thus considered the same as the one presented in (Landschützer et al., 2016).

The NN_{open} and NN_{coast} are all available at the same monthly temporal resolution but are applied at different spatial resolutions. While NN_{open} uses a 1°x1° resolution, the coastal $p\mathrm{CO_2}$ data product is constructed at a higher 0.25°x0.25° resolution to better capture the spatial heterogeneity of the coastal zone. Thus, in order to combine and compare the products at the same spatial resolution, we divided each 1°x1° grid cell of the open ocean into 16 equal 0.25°x0.25° bins . NN_{coast} combines observations from 1998 through 2015 using SOCATv4, whereas NN_{open} uses SOCATv5 data from 1982 through 2016. In this study, we constructed a climatological mean for the common period covered by both products (1998-2015). Despite the use of different versions of the SOCAT database used to generate the two $p\mathrm{CO_2}$ products (SOCATv4 vs SOCATv5) we expect little influence on our results, since most of the new data introduced into SOCATv5 compared to SOCATv4 were added in the later years and, in particular, 2016 which is excluded from our analysis. Figure 1 illustrates the temporal mean of all available $p\mathrm{CO_2}$ observations extracted from the SOCATv5 dataset for the 1998-2015 period.

Figure 2 shows the climatological mean $p\mathrm{CO_2}$ for both NN_{open} (Landschützer et al., 2016) and NN_{coast} (Laruelle et al., 2017). The data products rely on sea masks that lead to a common overlap area at the coastal-open ocean transition of roughly $42\mathrm{x}10^6$ km^2, reflecting the lack of a commonly recognized definition of the boundary between both environments. While the landward limit of the NN_{open} is located ~~on average at around~~ at 1° (~~or roughly 100km~~and therefore varies in km depending on the geographical position) off shore, NN_{coast} extends from the coastline to either 400km offshore or the 1000 m isobath, whichever is encountered first. The bathymetry used follows the SOCAT coastal definition (Pfeil et al., 2013) and excludes estuaries and inner water bodies (Laruelle et al., 2013, 2017). This overlap area is the subject of our error analysis described below.

2.2 Merging algorithm

The combination of the two data products takes place in three steps which are illustrated in Figure 3. In a first step, we divide the globe into a raster of coarse 30°x30° boxes starting at 90°N and 180°W. The large box size ensures that, even in remote regions, observations from both open ocean and coastal ocean are represented in the overlap area. We then investigate the overlap area for each raster box individually. In a second step, within each 30°x30° box, the pixels that are only covered by either NN_{open} or NN_{coast} are assigned their respective $p\mathrm{CO_2}$ value. In a third step, all pixels where open ocean and coastal ocean $p\mathrm{CO_2}$ products overlap, that is, all 0.25°x0.25° pixels with co-located $p\mathrm{CO_2}$ values in the open ocean and coastal ocean datasets, are identified. To assign a $p\mathrm{CO_2}$ value in this overlap area, we weight the open and coastal $p\mathrm{CO_2}$ estimates by their standard error relative to the SOCATv5 open and SOCATv5 coastal ocean datasets, respectively. We calculate the standard error at the scale of each 30°x30° raster, as at this larger scale regions enough observations are available to provide an error statistic. To implement this scheme, we first calculate the standard error on each 30°x30° box as:

$$\sigma_i = \frac{RMSE_i}{\sqrt{N_i}} \qquad (1)$$

where RMSE is the root mean square error of the open and coastal datasets with respect to the SOCATv5 gridded observations, N is the number of available gridded data from SOCATv5 available in a given 30°x30° raster box and the subscript i

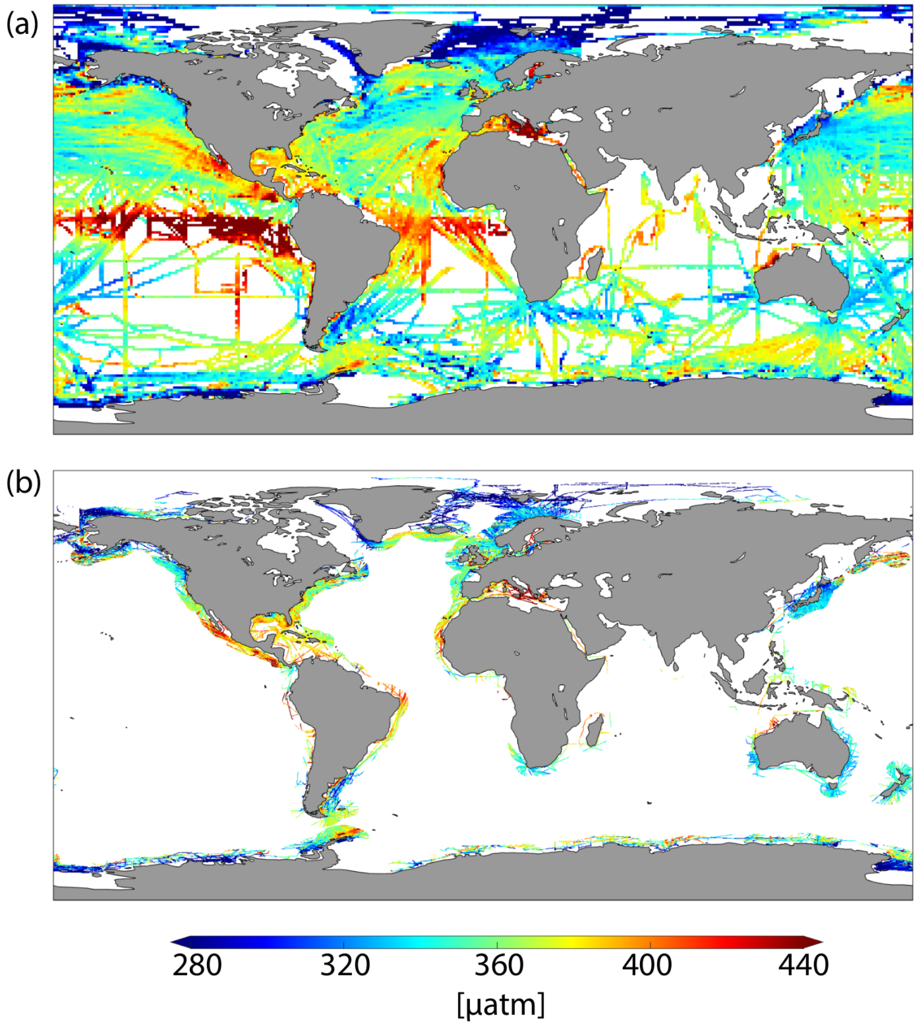

Figure 1. Gridded (a) 1° x1° open ocean and (b) 0.25° x0.25° coastal ocean $p\mathrm{CO}_2$ data values extracted from the SOCATv5 database from 1998 through 2015. Each value on the maps represents the mean of all values available within each grid cell for the period considered.

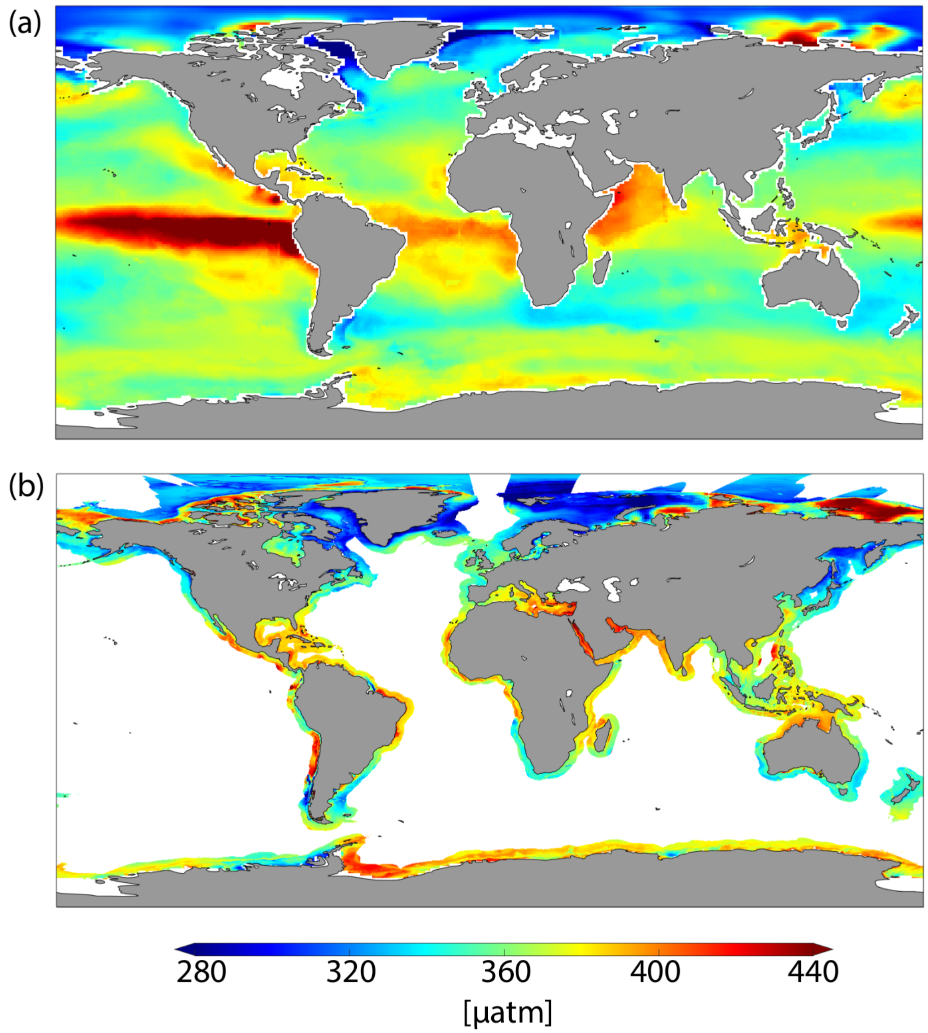

Figure 2. climatological mean of the (a) 1° x1° open ocean pCO_2 product by Landschützer et al. (2016) and (b) 0.25° x 0.25° the coastal ocean pCO_2 product by Laruelle et al. (2017) for the 1998-2015 period

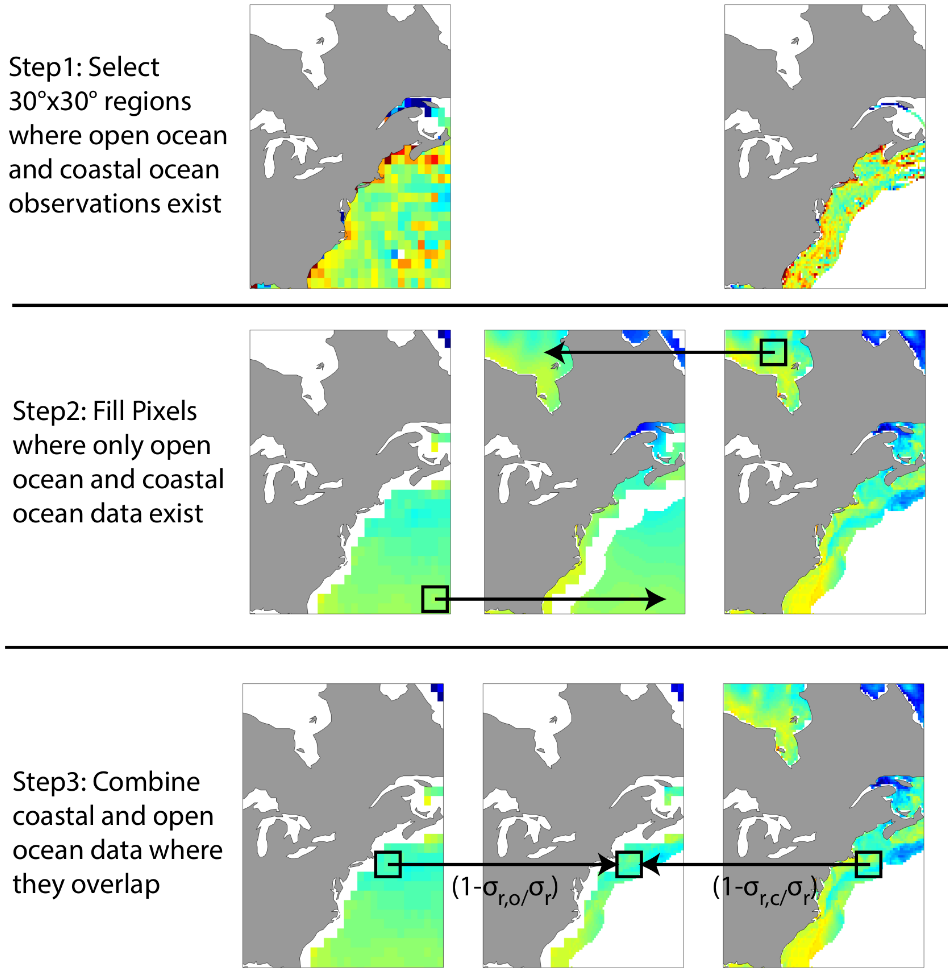

Figure 3. Schematic illustration of the merging steps. Step 1 shows an illustrative example of one 30°x30° box that includes both coastal and open ocean SOCAT observations. in Step 2 empty grid cells within the 30°x30° box are filled with coastal ocean as well as open ocean datapoints and in Step 3 open ocean and coastal ocean datapoints are combined where both exist.

refers to either NN$_{open}$ or NN$_{coast}$, respectively. Since we have simply divided the open ocean from a 1°x1° grid into 16 equal 0.25°x0.25° bins, we use an effective number of N^{eff}=N/16 for the open ocean. We do not account for autocorrelation in our calculations since we are only interested in the difference between the standard errors and assume autocorrelation lengths of similar magnitude between the SOCATv5 gridded datasets located in the coastal and open ocean domains, respectively. Next we calculate the total error for each 30°x30° degree raster region r as:

$$\sigma_r = \sigma_{r,o} + \sigma_{r,c} \tag{2}$$

and scale, for each grid-cell in the overlap area, the weight given to the open ocean and coastal ocean local pCO$_2$ value by the standard error of each raster region:

$$pCO_{2,overlap} = (1 - \frac{\sigma_{r,o}}{\sigma_r}) \cdot pCO_{2,o} + (1 - \frac{\sigma_{r,c}}{\sigma_r}) \cdot pCO_{2,c} \tag{3}$$

Substantial differences exist between the mean difference and standard deviations of NN$_{o}pen$ and NN$_{c}oast$ and the respective measurements from the SOCAT database within each 30°x30° degree raster. Figure 4 illustrates these differences. While both NN$_{o}pen$ and NN$_{c}oast$ have a near 0 bias for the mean difference, some rasters show differences exceeding 15μatm. While more variability appears in NN$_{c}oast$, this can largely be explained by to the overall smaller number of gridded measurements. The larger number of gridded measurements in NN$_{o}pen$ is a result from the division of the 1x1 degree cells into 16 quarter degree boxes. Therefore, we reduce the number of effective degrees of freedom for the open ocean by 16. To generate the final merged product we perform an additional smoothing using a 8x8 grid point running mean filter (roughly 200km by 200km at the equator).

3 Results and discussion

3.1 Large scale pCO$_2$ patterns along the coastal-open ocean continuum

The long term mean pCO$_2$ field at 0.25° resolution for NN$_{open}$ and NN$_{coast}$ is shown in Figure ~~4.~~ 5. In most oceanic regions, the transition from open to coastal ocean occurs without steep gradients, particularly in the subtropics ($\sim$ 20°N-50°N) of the northern hemisphere. However, exceptions exist in the tropics like the Peruvian upwelling system, the Namibian/Angolan coast in the South Atlantic and off Somalia and the Arabian Peninsula. Moreover, abrupt spatial gradients in pCO$_2$ have been observed in large river plumes such as that of the Amazon (Ibanhez et al., 2015) or on continental shelves influenced by large rivers. The identification of such gradients, however, results only from a first order visual inspection between the two products. In what follows, we perform a quantitative analysis of the merging procedure and of the resulting pCO$_2$ fields in the overlap area.

Figure ~~5~~ 6 reports the absolute pCO$_2$ difference in % between NN$_{coast}$ and NN$_{open}$ along the common overlap area relative to the mean partial pressure of the merged climatology. Figure ~~5~~ 6 shows a clear latitudinal pattern with the lowest difference in

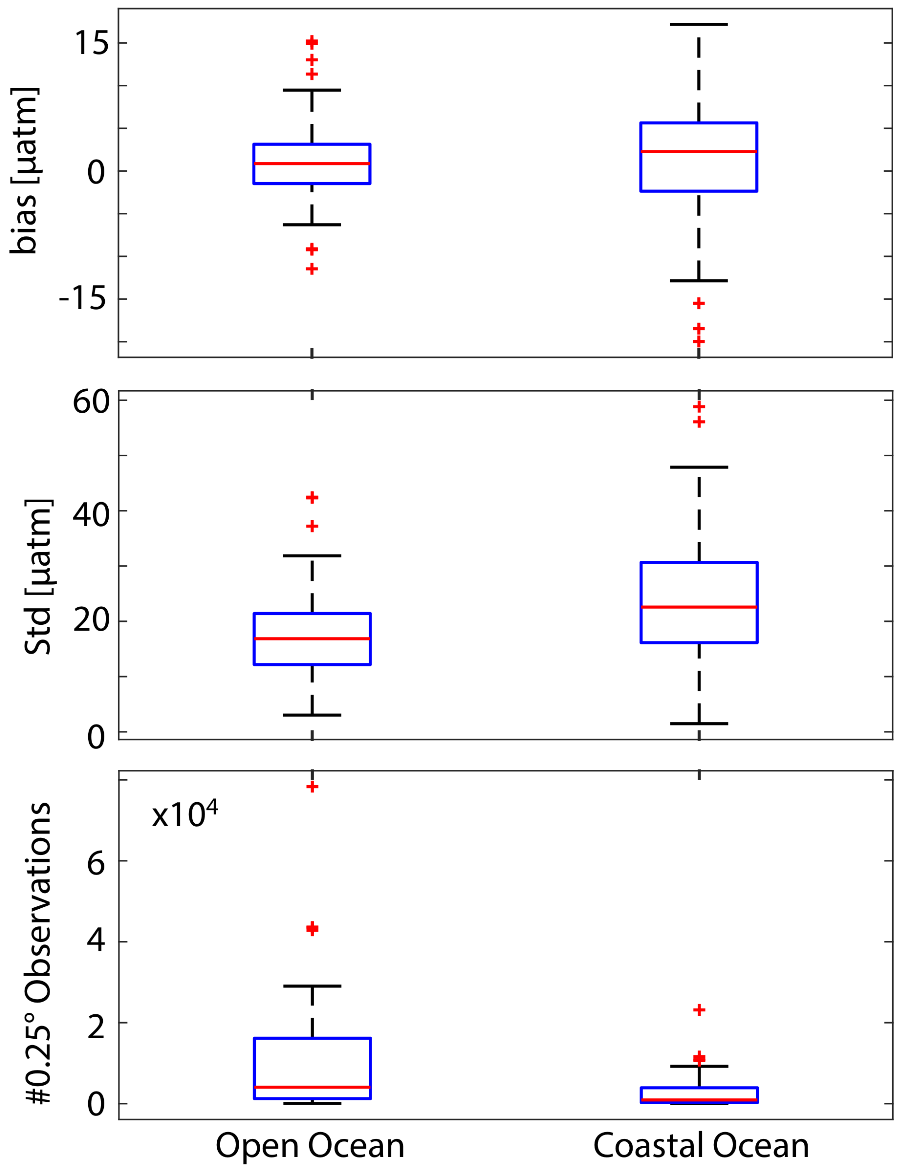

Figure 4. Box-Whisker plot of the mean difference (top), standard deviation (middle) and number of 0.25° pixels occupied with measurements (bottom) in the common overlap area for each 30°x30° box used for merging NN_{open} and NN_{coast}.

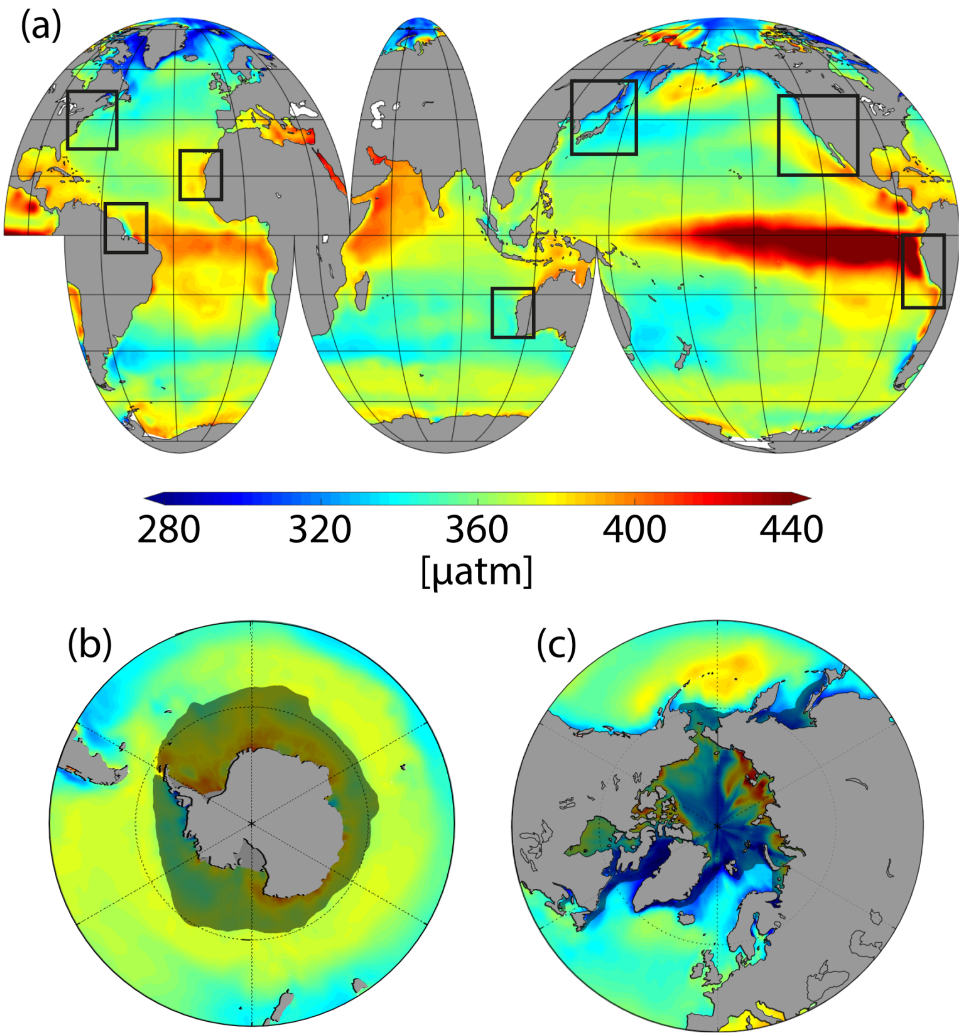

Figure 5. (a) climatological mean pCO_2 of the merged product presented in this study. Panels (b) and (c) highlight the polar regions. Black Boxes in (a) illustrate regions that are further investigated in the regional analysis. Shaded areas in (b) and (c) delineate the maximum sea ice extend.

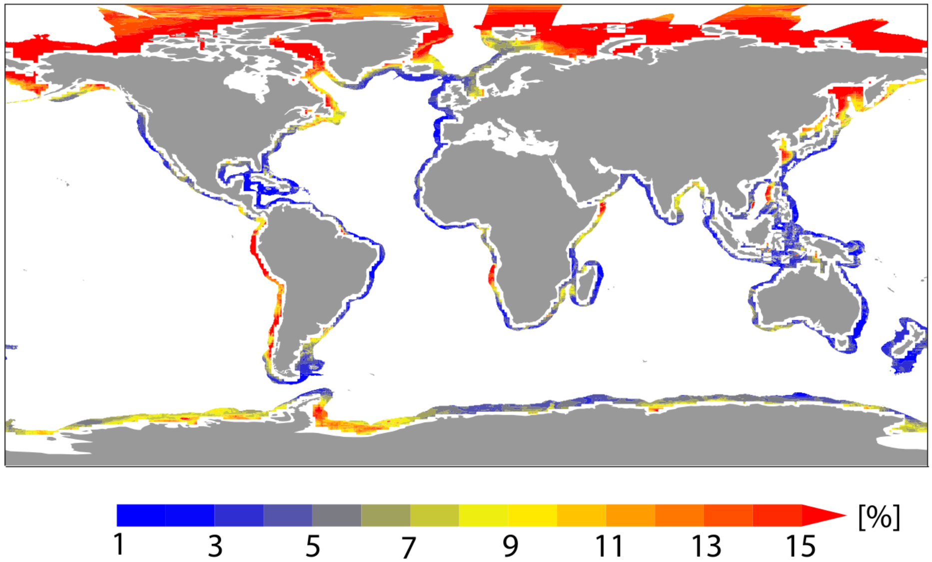

Figure 6. $p\mathrm{CO}_2$ mismatch between NN_{coast} and NN_{open} in the overlap area relative to the mean CO_2 partial pressure of the merged product. Blue colors indicate a mismatch below 5%, whereas red colors indicate a mismatch of more than 5%.

the low and subtropical latitudes and the largest differences in the high latitudes, especially in the northern hemisphere. We find in particular, that discrepancies are large in the newly added Arctic Ocean, but also in other seasonally ice-covered areas that have been previously described in NN_{open} and NN_{coast} publications (e.g. the Labrador Sea). One significant contributer to this difference might be that NN_{coast} uses information about seaice in reconstructing the surface ocean pCO_2. Acknowledging this discrepancy in seasonally ice-covered regions, we further focus our error analysis and products comparison on ice-free areas, based on the sea-ice product of Rayner et al. (2003). There are some exceptions to this general latitudinal trend consistent with our first qualitative inspection, such as along the Pacific coastline of South America, the African coast in the South Atlantic and the Arabian Sea, i.e. the regions with steep gradients already identified above. Furthermore, a gradient of decreasing $p\mathrm{CO}_2$ from the coast to the open ocean has been reported over the continental shelves of the Eastern US and Brazil (Laruelle et al., 2015; Arruda et al., 2015) and may exist in other regions as a consequence of the influence of rivers oversaturated in CO_2 combined with a limited estuarine filter (Laruelle et al., 2015). It is thus possible that the $p\mathrm{CO}_2$ predicted by the coastal SOM-FFN are slightly skewed towards higher values in some regions because of presence of overall higher $p\mathrm{CO}_2$ observations in the calibration data pool. While there is no clear basin-wide bias structure, systematic differences can be found regionally such as in the southeast Pacific Ocean and the Southern Ocean (south of 35°S). Overall, the largest relative differences are located in the overlap areas of the Arctic Ocean.

In spite of clear regional discrepancies, the mean difference, that is to say the bias, between the two estimates in the overlap area remains close to 0 μatm when integrated globally (table 1), whether or not the comparison is limited to the locations where observations exist (table 1 columns 1-3). Furthermore, the mismatch between the two products is in the range of the

Table 1. Mean error analysis (bias and RMSE) within the overlap area between NN_{coast} and NN_{open} and the observations from the SOCATv5 dataset . The comparison is performed for the total overlap area, the area fraction where no observations exist and the area covered by observations. The bias and RMSE between the $p\mathrm{CO}_2$ map products and the SOCATv5 open and coastal datasets are also reported.

	Coastal-open total	Coastal-open no obs.	Coastal-open colocated to obs.	Open-SOCAT	Coastal-SOCAT
Bias [μatm]	0.6	0.6	0.6	0.7	1.5
RMSE [μatm]	36.4	36.9	20.0	18.3	26.8

mismatch between the individual products and the available observations in SOCATv5. This result is a consequence of the neural network-based interpolation applied here at the global scale. In particular, the SOM-FFN is designed to minimize the mean squared error between available observations and the network output over the entire domain of application.

The global RMSE between NN_{open} and NN_{coast} as well as the SOCAT observations within the overlap area is in the range of previously reported global values by Landschützer et al. (2016) and Laruelle et al. (2017). In general, the spread between open ocean and continental coastal $p\mathrm{CO}_2$ varies more than the spread between coastal estimates and SOCAT or between open estimates and SOCAT, possibly indicating that the SOM-FFN method is having difficulties generalizing the $p\mathrm{CO}_2$ in the coastal-open ocean continuum.

3.2 Regional analyses of $p\mathrm{CO}_2$ field

A more detailed analysis is performed in the overlap of several regions selected to encompass a wide variety of conditions. These regions, indicated in Figure ~~4~~5, include three areas characterized by strong upwelling and offshore transport (Peruvian upwelling system, Canary upwelling system, US west coast) but contrasted data coverage, two data rich regions (Sea of Japan, US east coast) of which one comprises a marginal sea (Sea of Japan), one region where seasonal data are scarce (West Coast of Australia), and a region characterized by strong river outflow (Amazon river plume).

In order to further investigate the role of existing observations in upwelling regions we first focus on the Canary upwelling system and the Peruvian upwelling system. These two regions are part of the Eastern Boundary Upwelling Systems and subject to many ecosystem stressors, such as ocean acidification or deoxygenation (Gruber, 2011). Therefore, monitoring the full aquatic continuum is essential in these regions. Both are characterized by strong upwelling and significant offshore transport of carbon rich water from depth (see e.g. Lovecchio et al., 2018; Franco et al., 2018) resulting in elevated $p\mathrm{CO}_2$ levels exceeding atmospheric levels at the sea surface. Such values are consistent with observations in the Canary upwelling system (Figure ~~6~~7) extracted from either the open ocean SOCAT dataset (Bakker et al. (2016), Figure ~~6b~~7b) or the coastal SOCAT dataset (Bakker et al. (2016)Figure ~~6c~~7c) and, consequently, the merged $p\mathrm{CO}_2$ product (Figure ~~6a~~7a). Furthermore, the Canary upwelling system is well covered by both open ocean and coastal ocean observations. As a consequence - despite a few areas with larger differences - the overall mismatch between the coastal ocean and NN_{open} (figure ~~6d~~7d) is in the range of their relative mismatch towards the observations (see figure ~~6e-f~~7e-f) and generally within 10μatm.

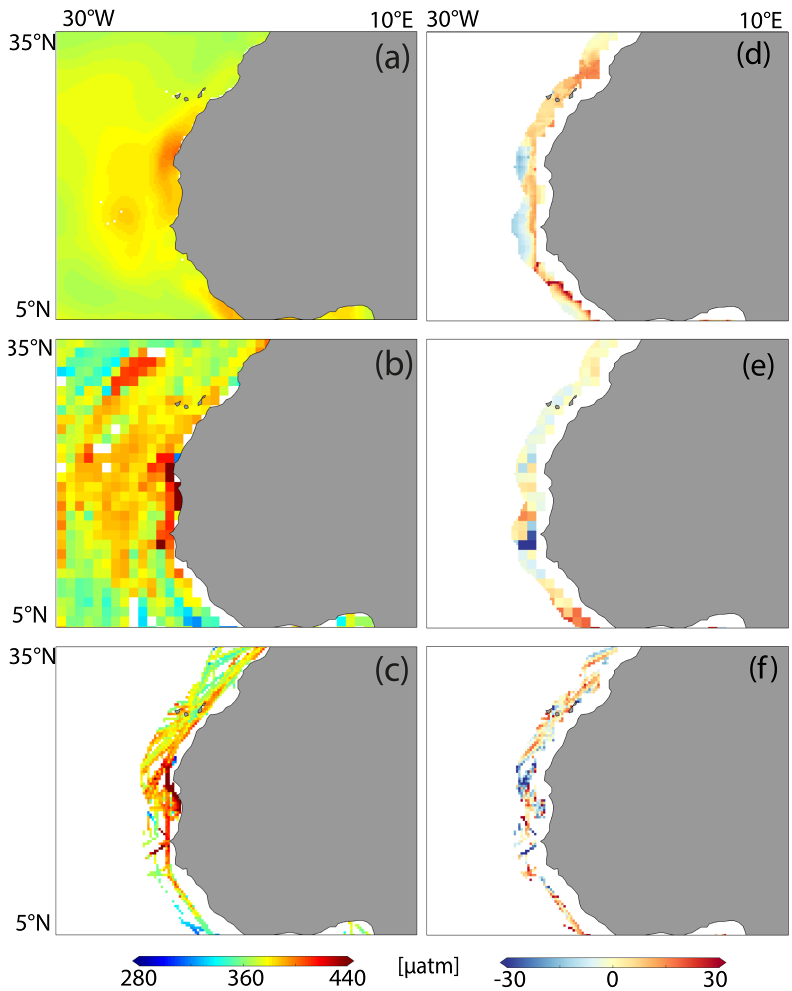

Figure 7. Mismatch analysis along the Canary upwelling region ~~from~~ for the 1998 through 2015 period. The climatological mean pCO_2 is reported for (a) the merged product, (b) all available SOCATv5 data for the open ocean, and (c) all coastal SOCATv5 data (as illustrated in Figure 1 for the global ocean). The pCO_2 mismatch is illustrated in (d) as the difference between NN_{coast} and NN_{open}. Panel (e) reports the mismatch between the NN_{open} and the SOCATv5 open ocean dataset along the overlap area while panel (f) reports the mismatch between the coastal product and the SOCATv5 coastal dataset along the overlap area.

In contrast to the Canary upwelling system, the Peruvian upwelling system shows a steep $p\mathrm{CO}_2$ gradient between the off-shore and near shore regions (Figure ~~7a~~8a), particularly just south of the equator. A closer inspection of the available observations (Figure ~~7b~~ 8b and c) reveals that, particularly in the near-shore domain at the equator, several of the few available observations of the sea surface $p\mathrm{CO}_2$ indicate low partial pressures resulting in a low reconstructed coastal $p\mathrm{CO}_2$, as already identified by Laruelle et al. (2017). The mismatch that results from the upscaling of the low $p\mathrm{CO}_2$ data in the coastal domain is further reflected in the difference between the coastal and open ocean $p\mathrm{CO}_2$ fields in the overlap area (figure ~~7~~ 8 d). The mismatch between the open ocean and NN_{coast} exceeds 30μatm and is larger than the difference between the individual products and the observations (figures ~~7~~ 8 e-f), suggesting that the disagreement between the open ocean and NN_{coast} in the overlap area stems from their data treatment. The fewer existing coastal observations of low $p\mathrm{CO}_2$ are extrapolated in space, spreading a potential mismatch over a larger area. Likewise, the near-shore domain in the NN_{open} is influenced by the high CO_2 partial pressures off-shore. This data sparsity and spatial heterogeneity is a further challenge for model evaluation Franco et al. (2018).

No steep $p\mathrm{CO}_2$ gradient can be identified along the west coast of Australia in the merged product (Figure ~~8~~9). The highest CO_2 partial pressures are found near shore along the Leeuwin current (Smith et al., 1991) and the lowest observed $p\mathrm{CO}_2$ can be found along the West Australian current. The area is spatially ~~well~~ covered both in the open and coastal ocean SOCAT datasets (Figure ~~8~~ 9 b and c) and therefore the overall difference towards observed values remains among the smallest of all investigated regions. This is remarkable given the lack of seasonal observations, which will be discussed in the subsequent section. NN_{open} and NN_{coast} agree with each other spatially within 15 μatm (figure ~~8d~~9d), which is in the range of the mismatch between the individual products and the respective SOCAT observations (figures ~~8~~ 9 e-f). Both products tend to overestimate the low $p\mathrm{CO}_2$ towards the South of the domain. This is reflected in the positive mismatch towards the SOCAT observations (Figure ~~8~~ 9 e and f) in the common overlap area where, the difference between the neural network estimates and the raw data exceeds 15 μatm for both products.

Observations in the Sea of Japan and adjacent Pacific Ocean suggest large variability in the $p\mathrm{CO}_2$ with the lowest observed values just north of the Korean peninsula and the highest observed $p\mathrm{CO}_2$ in the Yellow Sea (figures ~~9~~ 10 b-c). Furthermore, low $p\mathrm{CO}_2$ is also observed south of the island of Hokkaido. These large spatial variations in the $p\mathrm{CO}_2$ are also visible in the merged $p\mathrm{CO}_2$ product (figure ~~9a~~10a). A notable exception is the Korean Straight, where observations suggest a lower $p\mathrm{CO}_2$ than reconstructed. The strong variability in the observed $p\mathrm{CO}_2$ reflects the complex carbon dynamics in the Sea of Japan (Chen et al., 1995; Park et al., 2006), which is also reflected in the larger mismatch between products and towards the SOCAT observations (figures ~~9~~ 10 d-f). The disagreement may indicate that the global scale NN_{open} and NN_{coast} products are not particularly skilled in representing the strong regional dynamics of marginal sea. A better agreement between the neural network reconstructions and observations is found in the Pacific Ocean east of the Japanese islands, where the merged estimate also reveal a better agreement between NN_{open} and NN_{coast} (Figure ~~9~~ 10 d) and low biases in the range of 5 μatm towards SOCAT observations (Figure ~~9~~ 10 e and f).

Some of the best monitored regions spanning both coastal and near-shore open ocean can be found along the US coast ~~(Fennel et al., 2008; Laruelle et al., 2015; Fennel et al., 2019)~~(Fennel et al., 2008; Signorini et al., 2013; Laruelle et al., 2015; Fennel et al

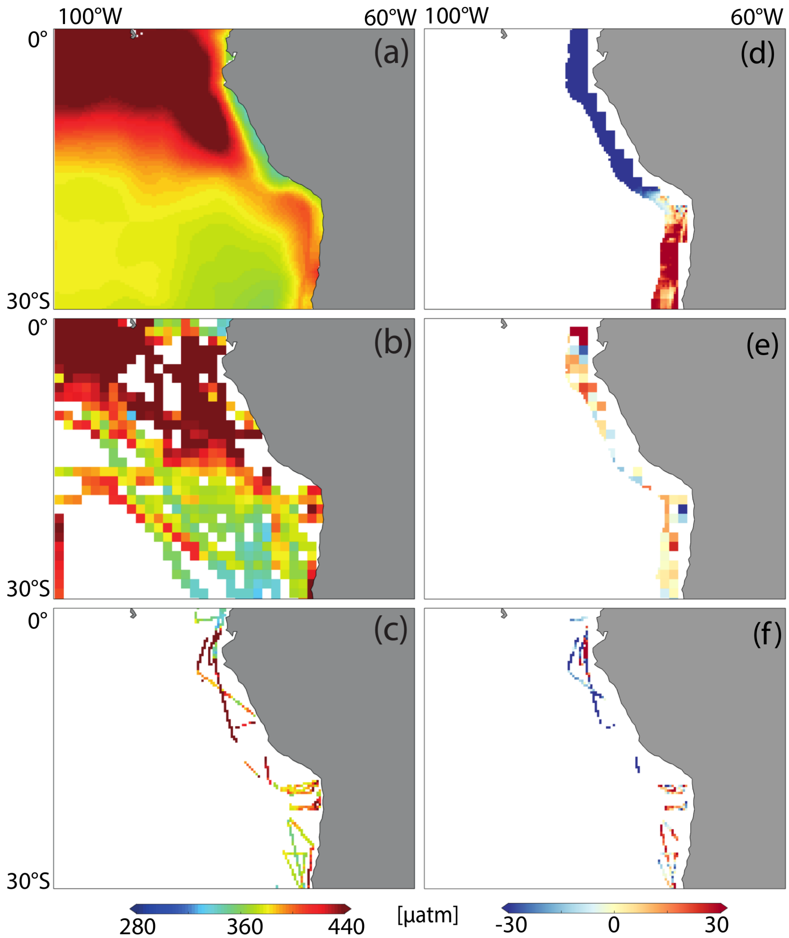

Figure 8. ~~Like Figure 6 but for~~ Mismatch analysis along the Peruvian upwelling ~~system~~region for the 1998 through 2015 period. The climatological mean pCO_2 is reported for (a) the merged product, (b) all available SOCATv5 data for the open ocean, and (c) all coastal SOCATv5 data (as illustrated in Figure 1 for the global ocean). The pCO_2 mismatch is illustrated in (d) as the difference between NN_{coast} and NN_{open}. Panel (e) reports the mismatch between the NN_{open} and the SOCATv5 open ocean dataset along the overlap area while panel (f) reports the mismatch between the coastal product and the SOCATv5 coastal dataset along the overlap area.

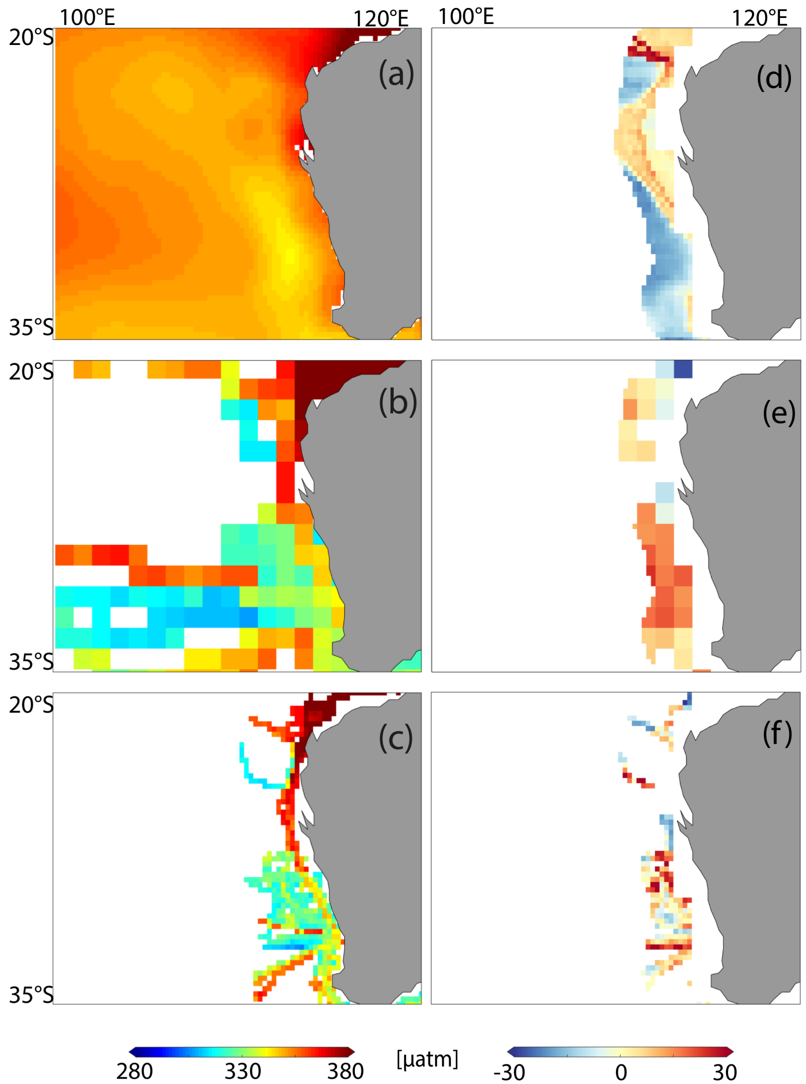

Figure 9. ~~Like Figure 6 but for~~ Mismatch analysis along the Australian west coast region for the 1998 through 2015 period. The climatological mean pCO$_2$ is reported for (a) the merged product, (b) all available SOCATv5 data for the open ocean, and (c) all coastal SOCATv5 data (as illustrated in Figure 1 for the global ocean). The pCO$_2$ mismatch is illustrated in (d) as the difference between NN$_{coast}$ and NN$_{open}$. Panel (e) reports the mismatch between the NN$_{open}$ and the SOCATv5 open ocean dataset along the overlap area while panel (f) reports the mismatch between the coastal product and the SOCATv5 coastal dataset along the overlap area.

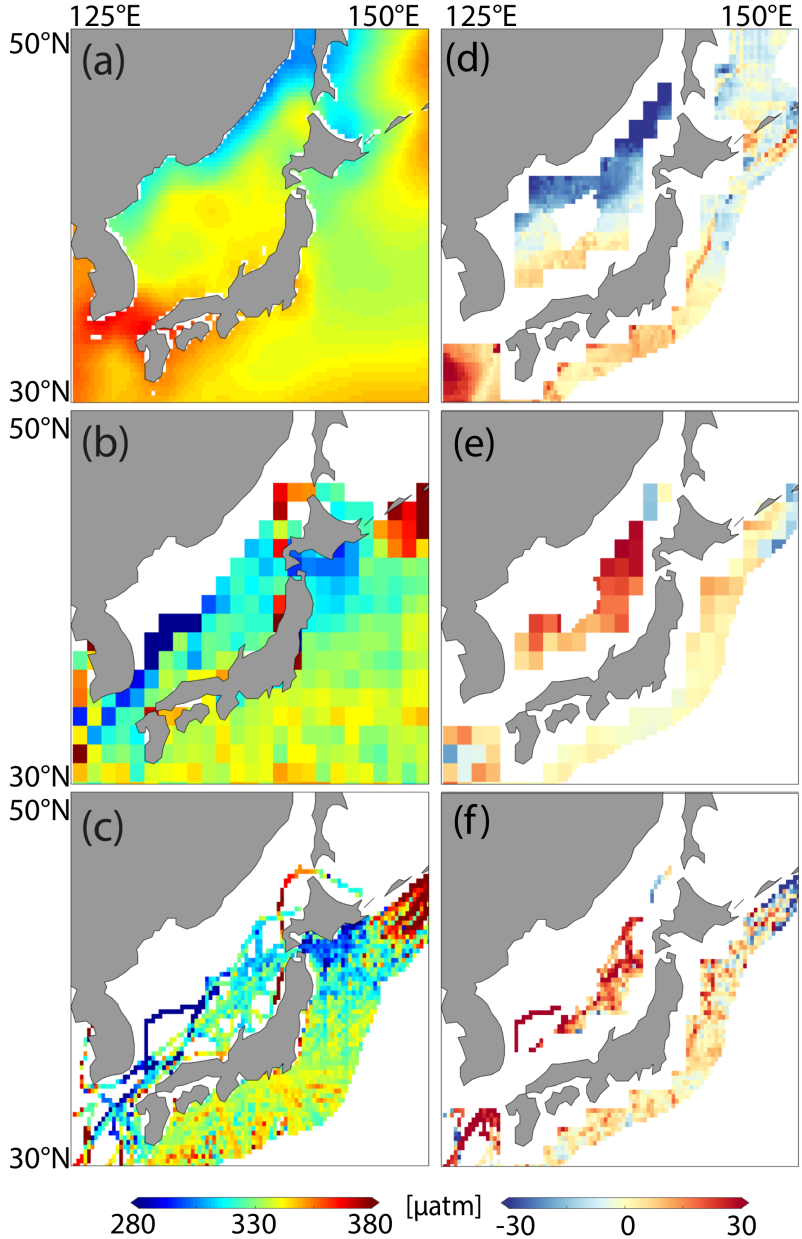

Figure 10. ~~Like Figure 6 but for~~ Mismatch analysis along the Sea of Japan region for the 1998 through 2015 period. The climatological mean $p\mathrm{CO_2}$ is reported for (a) the merged product, (b) all available SOCATv5 data for the open ocean, and (c) all coastal SOCATv5 data (as illustrated in Figure 1 for the global ocean). The $p\mathrm{CO_2}$ mismatch is illustrated in (d) as the difference between NN_{coast} and NN_{open}. Panel (e) reports the mismatch between the NN_{open} and the SOCATv5 open ocean dataset along the overlap area while panel (f) reports the mismatch between the coastal product and the SOCATv5 coastal dataset along the overlap area.

. Indeed all 1x1° open ocean and almost all 0.25°x0.25° coastal pixels are filled with raw observations off the eastern US coastline. While the mean of all observed $p\mathrm{CO_2}$ values from SOCAT (Figure ~~10b~~ 11b and c) suggests substantial regional variability, the merged estimate (Figure ~~10a~~11a) is, as a result of the neural network interpolation algorithm, substantially smoother. In particular, the lower latitudes (25-35°N, Figure ~~10e~~ 11e and f) are well reconstructed by the neural network algorithms in both open and coastal ocean domains. Larger discrepancies however exist in the higher latitudes (35-45°N, Figure ~~10e~~ 11e and f). Landschützer et al. (2014) attributed ~~this~~ a larger mismatch to the complex biogeochemical dynamics of the Gulf Stream region, where the measured $p\mathrm{CO_2}$ is ~~overestimated~~ underestimated by both the open and coastal ~~estimates. The~~ products. The strong mesoscale dynamics and the influence of the cold Labrador current in this region are not well represented in the rather coarse 0.25° NN_{coast} and 1° NN_{open} products. The smooth transition between coastal and open ocean in Figure ~~10a~~ 11a indeed suggests that the intensively surveyed US east coast aquatic continuum can be well reconstructed by combining the open ocean and coastal ocean $p\mathrm{CO_2}$ datasets.

Similarly well monitored to the US east coast is the US west coast upwelling system, not the least because its variability is tightly linked to El Nino Southern Oscillation (see e.g. Lynn and Bograd, 2002; Frischknecht et al., 2015). Here, we find an overall good agreement between NN_{coast} and NN_{open}. The agreement in the overlap area of the merged product (Figures ~~11d~~12d) is among the best reported globally. Interestingly, near shore, the merged estimate (Figure ~~11a~~12a) reveals a lower mean $p\mathrm{CO_2}$ than suggested from both the open ocean and coastal ocean SOCAT datasets (figure ~~11~~ 12 b and c). The small error compared to the SOCAT observations suggests that this is not the result of the 2 products being in disagreement but might relate to ~~the climatological nature of the merged product, which does not reflect the variable~~ changes in upwelling as a result of interannual variability linked to ENSO events that are not well captured by the merged product.

Finally, we investigate the spatial structure of the reconstructed $p\mathrm{CO_2}$ from a region typically dominated by the freshwater outflow of a large river mouth, i.e. the Amazon outflow in the tropical Atlantic Ocean (Figure ~~12~~13). Studies linking circulation with the local $\mathrm{CO_2}$ dynamics are sparse (Ibanhez et al., 2015; Lefevre et al., 2013). Very few observations exist, particularly in the near-shore region (Figure ~~12b-c~~13b-c). Nevertheless, studies suggest that the Amazon river outflow becomes a significant $\mathrm{CO_2}$ sink when it mixes with ocean waters (Lefevre et al., 2010). The strong variance in observed $p\mathrm{CO_2}$ (Bakker et al., 2016) provides a challenge for any algorithm to reconstruct the full $p\mathrm{CO_2}$ field in such region. Nevertheless, both coastal and oceanic data products are in good agreement (Figure ~~12d~~13d) with the exception of the area under direct influence of Amazon River outflow. This difference potentially stems from the NN_{open} being unable to associate the $p\mathrm{CO_2}$ variability observed in this area to the strong salinity gradients, which is better represented in the coastal ocean $p\mathrm{CO_2}$ product. Both products show differences of similar magnitude when compared to the SOCAT observations (Figure ~~12e-f~~13e-f) and similar error structures as both products overestimate the $p\mathrm{CO_2}$ in the northern and underestimate the $p\mathrm{CO_2}$ in the southern sections of the overlap area.

While global errors between the data products and observations remain low (see table 1), figures ~~6-12~~ 7-13 show that, at the regional scale, larger differences emerge. We therefore expend our standard error statistics as presented in table 2 for the selected regions. Overall, we find at the regional level that the inter-product mismatch, represented by the bias, is substantially larger than in the global analysis but does not exceed $\sim$8μatm with one prominent exception: the Peruvian upwelling system where the mismatch reaches 14.8 μatm. Here, the substantial disagreement between the two products results from the underes-

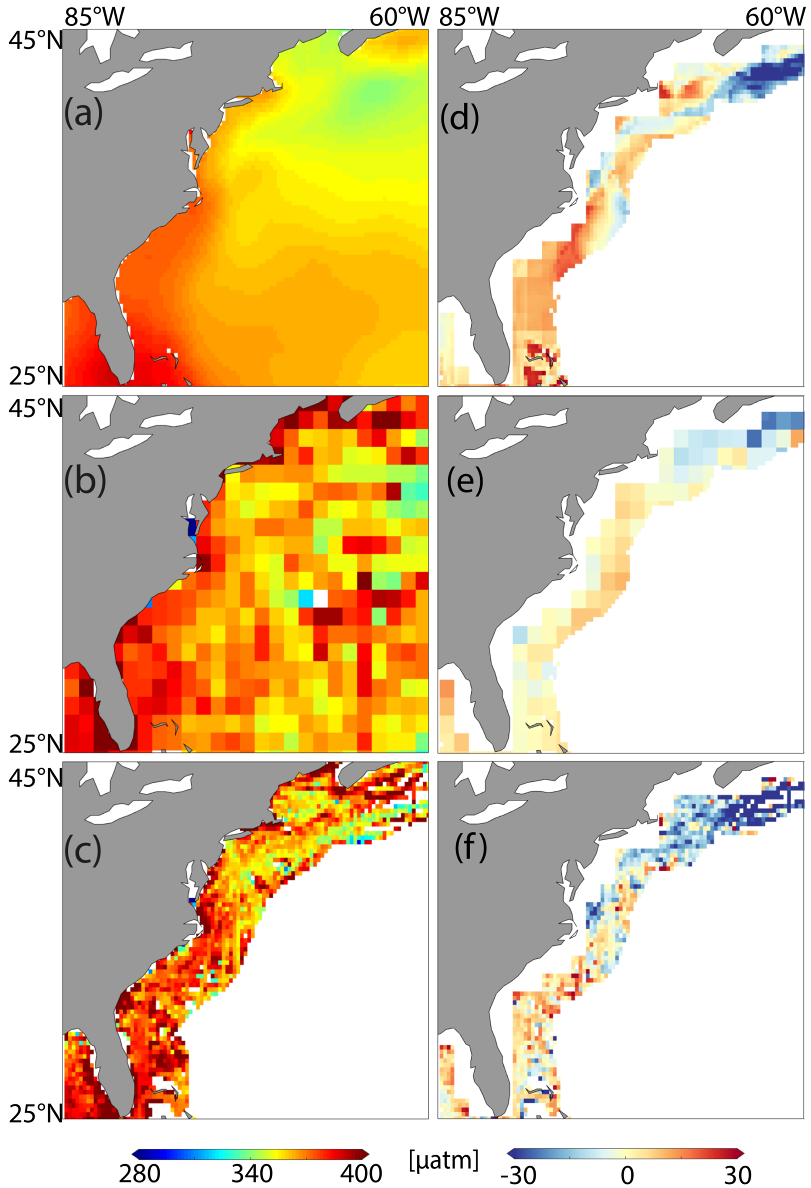

Figure 11. ~~Like Figure 6 but for~~ Mismatch analysis along the ~~US~~ United States east coast for the 1998 through 2015 period. The climatological mean pCO_2 is reported for (a) the merged product, (b) all available SOCATv5 data for the open ocean, and (c) all coastal SOCATv5 data (as illustrated in Figure 1 for the global ocean). The pCO_2 mismatch is illustrated in (d) as the difference between NN_{coast} and NN_{open}. Panel (e) reports the mismatch between the NN_{open} and the SOCATv5 open ocean dataset along the overlap area while panel (f) reports the mismatch between the coastal product and the SOCATv5 coastal dataset along the overlap area.

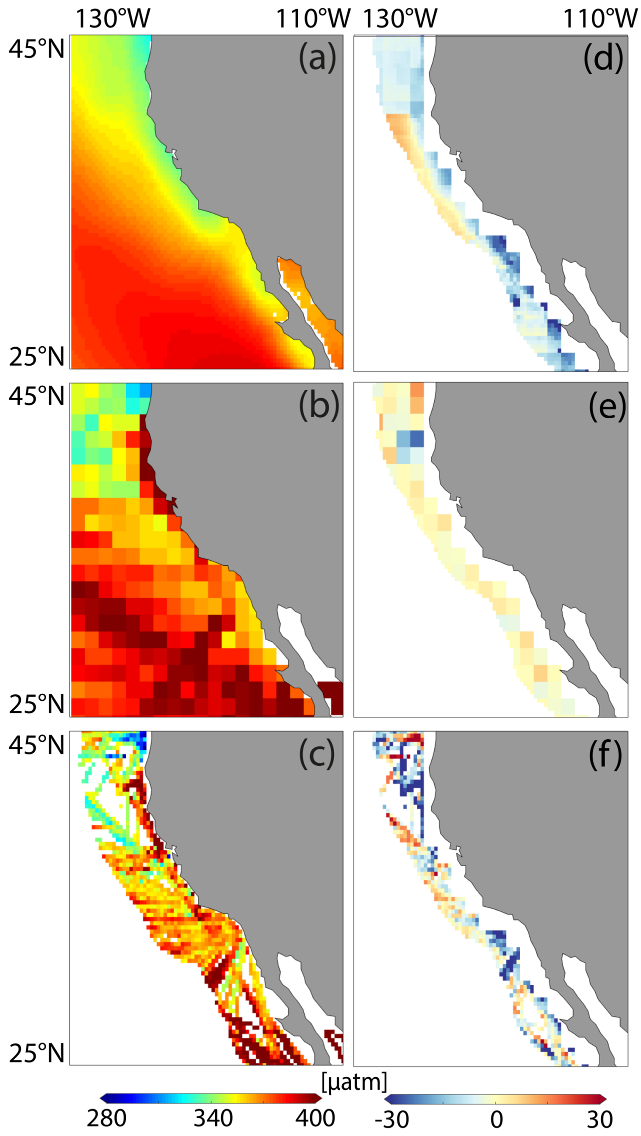

Figure 12. ~~Like Figure 6 but for~~ Mismatch analysis along the ~~US~~ United States west coast for the 1998 through 2015 period. The climatological mean $p\mathrm{CO_2}$ is reported for (a) the merged product, (b) all available SOCATv5 data for the open ocean, and (c) all coastal SOCATv5 data (as illustrated in Figure 1 for the global ocean). The $p\mathrm{CO_2}$ mismatch is illustrated in (d) as the difference between NN_{coast} and NN_{open}. Panel (e) reports the mismatch between the NN_{open} and the SOCATv5 open ocean dataset along the overlap area while panel (f) reports the mismatch between the coastal product and the SOCATv5 coastal dataset along the overlap area.

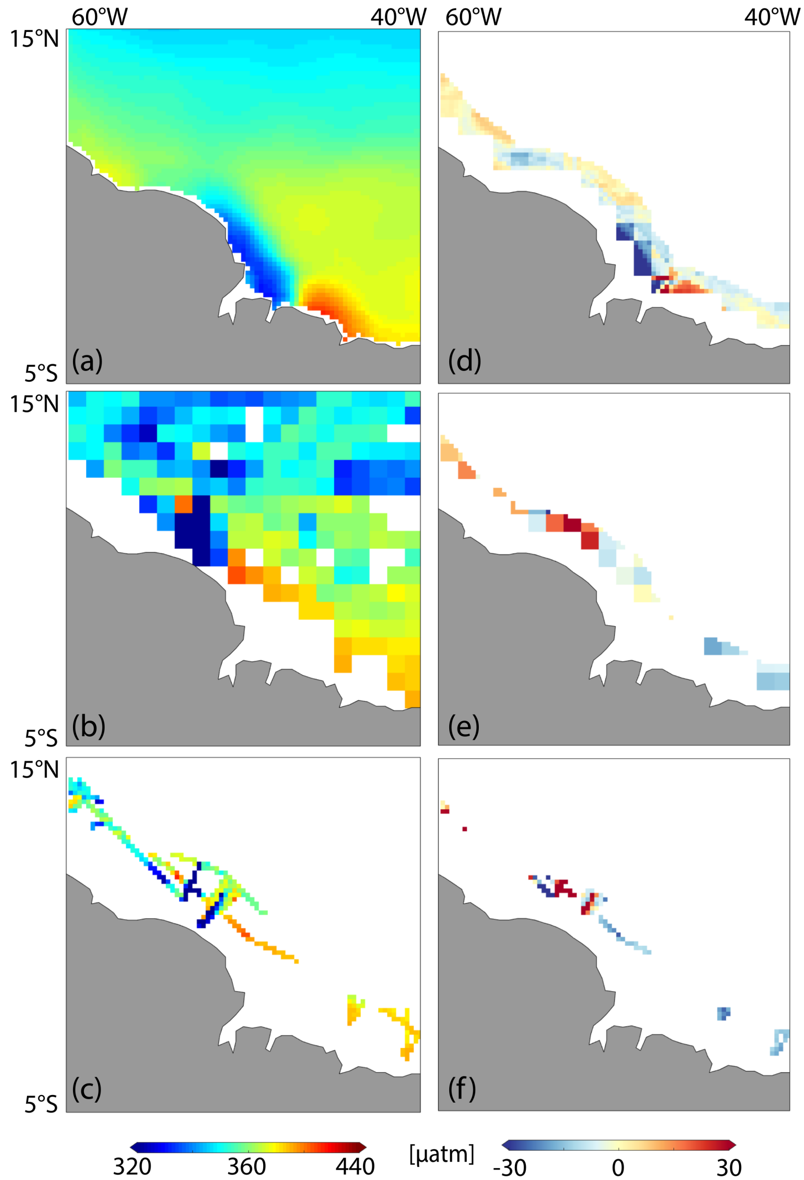

Figure 13. ~~Like Figure 6 but for~~ Mismatch analysis along the Amazon outflow region for the 1998 through 2015 period. The climatological mean pCO_2 is reported for (a) the merged product, (b) all available SOCATv5 data for the open ocean, and (c) all coastal SOCATv5 data (as illustrated in Figure 1 for the ~~tropical Atlantic Ocean~~global ocean). The pCO_2 mismatch is illustrated in (d) as the difference between NN_{coast} and NN_{open}. Panel (e) reports the mismatch between the NN_{open} and the SOCATv5 open ocean dataset along the overlap area while panel (f) reports the mismatch between the coastal product and the SOCATv5 coastal dataset along the overlap area.

Table 2. Mean error analysis (bias and RMSE) within the overlap area between NN_{open} and NN_{coast} and the observations from the SOCATv5 dataset (Bakker et al., 2016) for 7 oceanic regions. The comparison is performed for the total overlap area, the area fraction where no observations exist and the area covered by observations. The biases and RMSE between pCO$_2$ products and SOCATv5 datasets are also reported for the open ocean and coastal ocean.

Region	Coastal-open total bias (RMSE) [μatm]	Coastal-open no obs. bias (RMSE) [μatm]	Coastal-open colocated to obs. bias (RMSE) [μatm]	Open-SOCAT bias (RMSE) [μatm]	Coastal-SOCAT bias (RMSE) [μatm]
Canary upwelling system (5-35°N)	3.6 (20.3)	3.8 (20.5)	-1.0 (16.3)	-0.6 (16.3)	-1.3 (24.6)
Peru upwelling system (0-30°S)	-34.3 (80.6)	-34.3 (80.7)	-14.8 (42.0)	2.2 (23.0)	-12.9 (49.0)
Australia west coast (20-35°S)	-3.4 (25.2)	-3.4 (25.3)	-7.6 (16.8)	8.5 (17.4)	4.1 (16.5)
Sea of Japan (30-50°N)	-3.5 (34.5)	-4.2 (35.8)	2.4 (18.6)	2.0 (16.5)	4.5 (25.3)
US east coast (25-45°N)	1.7 (26.0)	2.4 (26.6)	-3.8 (21.1)	-0.1 (17.4)	-3.5 (27.9)
US west coast (25-45°N)	-7.5 (20.6)	-7.6 (20.7	-6.5 (19.6)	0.1 (13.7)	-7.0 (27.5)
Amazon outflow (5°S-15°N)	-5.5 (29.0)	-5.5 (29.0)	-0.5 (22.3)	11.2 (37.9)	14.8 (59.0)

timation of the coastal observations in the overlap domain by the coastal ocean pCO$_2$ product already shown by Laruelle et al. (2017).

We find that the bias between NN_{open} and NN_{coast} in the overlap area are larger where they are not co-located to observations (Table 2). The error spread between NN_{open} and NN_{coast}, represented by the RMSE, is likewise larger in areas where fewer observations exist (contrast column 1 and 2 in Table 2). Exceptions include the US east Coast and the West coast of Australia possibly linked to the larger mismatch of the individual products towards the respective SOCAT observations at these locations. Results from both products in the Amazon outflow region, in the US east coast for NN_{coast} and in the west coast of Australia for NN_{open} show a larger bias towards the SOCAT observations than the respective inter-model bias, illustrating that both methods generalize well. This further suggests that the estimates are locally constrained by information outside the investigated domain, which is possible considering the spatial distributions of the biogeochemical provinces generated by the SOM.

3.3 Seasonality

A further analysis in the selected regions aims to investigate the seasonal differences in pCO$_2$ between the original data products, the merged product, and observations (Figure ~~13~~14). In particular, we investigate the extent to which the mean biases reported above can be explained by seasonal differences in $p\mathrm{CO}_2$ among the different products. To this end, we average all months from 1998 through 2015 to create a seasonal climatology from our $p\mathrm{CO}_2$ products, without correction to a nominal reference year. We repeat this procedure for the SOCAT datasets, likewise without any corrections but being aware that this could lead to a sampling bias in the observed climatology. This approach is justified because we lack knowledge about the short-term variability in the observed carbon cycle and it is thus unclear on how such a correction would improve the representation of the observed $p\mathrm{CO}_2$ field.

In spite of the lack of seasonal sampling bias corrections, our analysis displays, for most regions, a close correspondence within a few μatm between open ocean and coastal ocean $p\mathrm{CO}_2$ data from SOCAT within the overlap area (blues and yellow bars in Figure ~~13~~14) with deviations mostly arising in the Peruvian upwelling system and the Amazon outflow regions where monthly differences can exceed 10 μatm. The good correspondence is expected to some degree because both datasets share a large fraction of the data. The analysis shows that the seasonality of the neural network-based on NN_{open} and NN_{coast} satisfactorily reproduce the seasonal fluctuations obtained directly from the raw data, highlighting that the reconstructed seasonal cycle is well constrained by the existing observations. Monthly deviations between the products largely stay within 10 μatm. An exception is the Sea of Japan in boreal winter, where NN_{open} overestimates the surface ocean $p\mathrm{CO}_2$ values recorded in the SOCAT data. All but three of the selected regions have full seasonal data coverage. The three regions without full coverage are the West coast of Australia, the Amazon outflow region and the Peruvian upwelling system. Despite the lack of seasonal observations along the West coast of Australia, both products agree well with regards to the seasonal cycle and differences stay within of 8-10μatm between the different products. Likewise, the otherwise good agreement between coastal ocean and open ocean estimate breaks down in the boreal summer in the Amazon outflow region, despite the lack of strong seasonality in the tropical latitudes.

The largest mismatch between data products and observations exist along the Peruvian upwelling system, where monthly differences between open ocean and coastal ocean estimates exceed 40μatm. Both estimates however show similar seasonal variability. The seasonal analysis further reveals that from all investigated regions, the Peruvian upwelling system shows the largest monthly differences between open ocean and coastal ocean SOCAT observations, with e.g. mean differences in March exceeding 30μatm between the open ocean and coastal ocean SOCAT datasets (Bakker et al., 2016). Furthermore, the largest observed partial pressures in NN_{open} appear in August where no data are available in the coastal ocean SOCAT dataset, highlighting that NN_{open} draws information from observations further away from shore during this month.

4 Data availability

The merged climatology (Landschützer et al. (2020), doi: 10.25921/qb25-f418) is available from NCEI OCADS and can be accesed via: https://www.nodc.noaa.gov/ocads/oceans/MPI-ULB-SOM_FFN_clim.html. NN_{open} is available vie NCEI OCADS and is accessible online https://www.nodc.noaa.gov/ocads/oceans/SPCO2_1982_present_ETH_SOM_FFN.html. NN_{coast} description and dataset can be downloaded from the following url: https://www.biogeosciences.net/14/4545/2017/

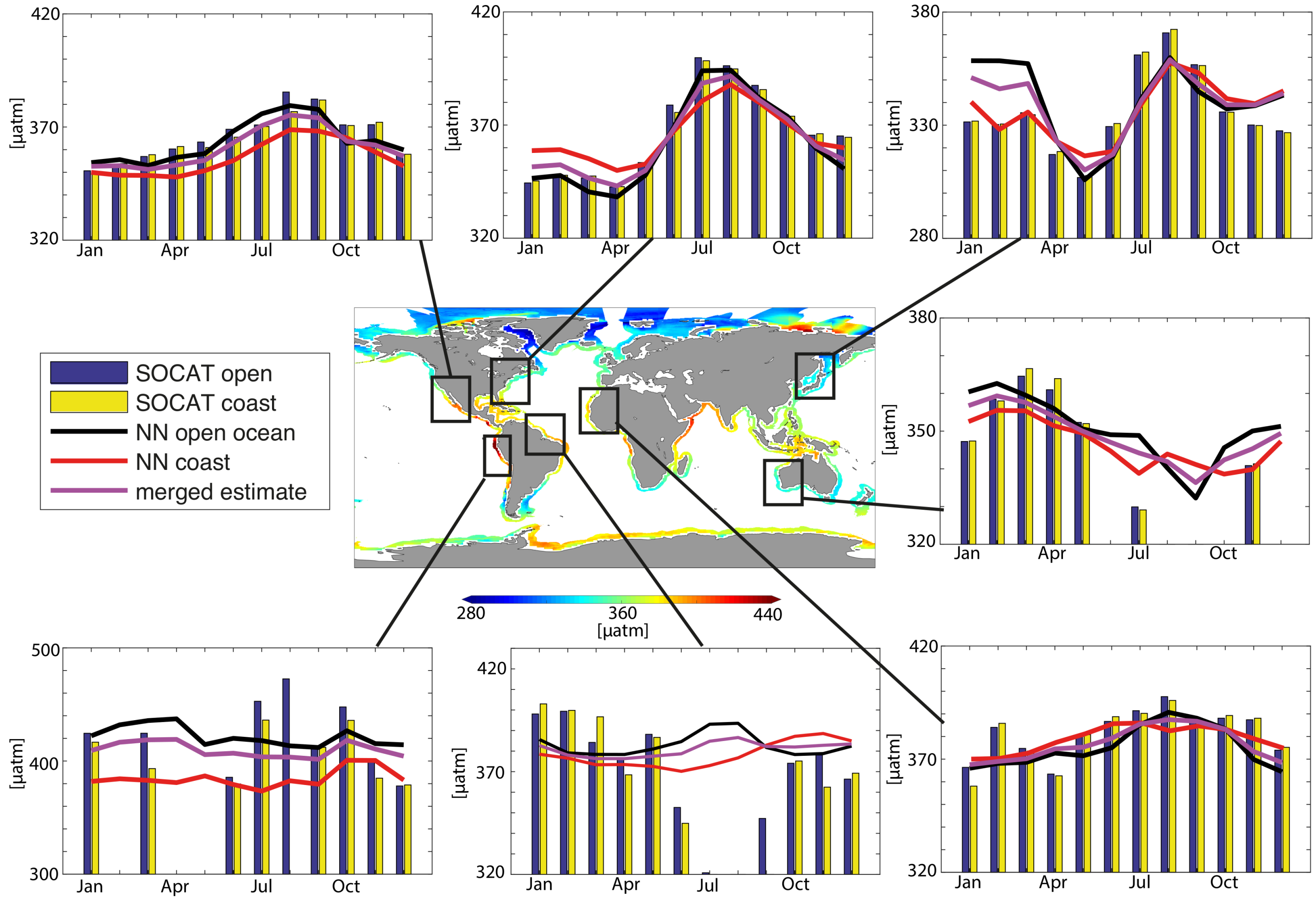

Figure 14. Seasonal pCO_2 cycle for the seven regions discussed in the text and highlighted in the center map. The seasonal cycles include a comparison of the monthly mean SOCAT observations without any interpolation (blue and yellow bars) as well as the open ocean (blue line), coastal ocean (red line) and merged (magenta line) reconstructions based on the respective SOCAT observations.

5 Conclusions

In this analysis, we combined two recently published sea surface pCO$_2$ products, covering the open ocean and the coastal domain. While the spatial coverage of NN$_{open}$ includes all surface waters located further than 1° off the coast, the spatial coverage of the NN$_{coast}$ includes surface waters until 400km off the coast, leading to ~~a roughly~~ an overlap domain of roughly 300km ~~wide overlap domain~~ close to the equator and increasing in extend towards the poles around the land surface. The common overlap area was used to compare both reconstructed pCO$_2$ estimates at regional to global scale and whether the observed agreement/disagreement is linked to data availability.

Our results show that, for most of the global ocean and particularly the subtropical latitudes in the northern hemisphere, NN$_{open}$ and NN$_{coast}$ agree well within the overlap domain. However, stronger differences exist in other parts of the world, particularly in the Peruvian upwelling system, the Arctic and Antarctic, the African coastline in the South Atlantic and the Arabian Sea, where fewer observations exist. Additionally, we find larger discrepancies in the marginal Sea of Japan. In other regions without complete seasonal data coverage such as the west coast of Australia, however, both products compare well. We therefore conclude that the lack of data coverage in combination with biogeochemical complexity triggered by upwelling, river influx or seasonal ice coverage contribute both to the mismatch. Additionally, methodological differences between NN$_{open}$ and NN$_{coast}$, such as differences in predictor data result in local differences, e.g. in ice covered regions where NN$_{coast}$ relies on sea-ice as predictor or shallow, stratified waters, where mixed layer depth serves as important proxy in NN$_{open}$. Closer inspection reveals that for most of the overlap regions, the difference between the open ocean and coastal ocean estimates falls within the range of the difference between NN$_{open}$ and NN$_{coast}$ and the respective SOCAT dataset from which they were created. Therefore, the combined pCO$_2$ climatology is not only a step forward in including the full oceanic domain with all its complexity into carbon budget analyses, but also help identify areas where additional continuous observations are critically needed to close current knowledge gaps.

Another way forward to further reduce the bias between the coastal and open ocean estimates would be to reconsider the cut-off definition between the two domains. Data sparse and often strongly variable regions such as the Peruvian upwelling system are very sensitive to the data selected to generate the pCO$_2$ fields. The ~~proposed overlap analysis~~ overlap analysis proposed here and particularly the Percent mismatch and RMSE analysis, further serves as a benchmark on how well we understand the coastal-to-open ocean continuum and its spatial variability and where we still lack essential measurements to close the gap between existing estimates, such as e.g. the Peruvian upwelling system or the seasonally ice-covered high latitude regions, in particular the Arctic Ocean. A next step should include the reduction of the mismatch between coastal and open ocean estimates in order to combine the two. This is an essential step towards an observation-driven global carbon budget. Closing such gap requires however close collaborations between open ocean and coastal ocean carbon cycle scientists in the future and be considered of high importance.

Finally, we introduced a new concept where we can locally evaluate the upscaling of existing measurements based on a common overlap region. In this study, we focused on mean differences and seasonal climatologies at regional and global scales. We find an encouraging agreement between seasonal cycles which gives us confidence that the existing products might be suitable to be applied to study lower frequency signals such as trends and interannual variability. Understanding of how differences in trends and inter-annual variabilities between the coastal and open oceans emerge and how they are linked to data availability should be a next step. Such analysis is essential to gain confidence in observational constraints and to find ways to further improve them in order to close the global carbon budget based on observations and provide data products form model benchmarking. Our approach can also be used to compare other overlapping datasets at a time when advanced interpolation techniques are yielding more and more oceanic data products with different spatial extensions and boundaries. Our study is therefore an important step towards a truly representative global ocean observation-based CO_2 product that includes all ocean domains.

Competing interests. We declare no competing interests

Acknowledgements. PL is supported by the Max Planck Society for the advancement of Science. The research leading to these results has received funding from the European Community's Horizon 2020 project under grant agreement no. 821003 (4C). GGL is research associate of the F.R.S-FNRS at the Universite Libre de Bruxelles. PR received funding from the VERIFY project from the European Union Horizon 2020 research and innovation program under grant agreement No. 776810. This study benefited from discussions with K. Six from the Max Planck Institute for Meteorology. The Surface Ocean CO2 Atlas (SOCAT) is an international effort, supported by the International Ocean Carbon Coordination Project (IOCCP), the Surface Ocean Lower Atmosphere Study (SOLAS), and the Integrated Marine Biogeochemistry and Ecosystem Research program (IMBER), to deliver a uniformly quality-controlled surface ocean CO2 database. The many researchers and funding agencies responsible for the collection of data and quality control are thanked for their contributions to SOCAT.

References

Arruda, R., Calil, P. H. R., Bianchi, A. A., Doney, S. C., Gruber, N., Lima, I., and Turi, G.: Air-sea CO2 fluxes and the controls on ocean surface pCO2 seasonal variability in the coastal and open-ocean southwestern Atlantic Ocean: a modeling study, Biogeosciences, 12, 5793–5809, https://doi.org/10.5194/bg-12-5793-2015, 2015.

Bakker, D. C. E., Pfeil, B., Smith, K., Hankin, S., Olsen, A., Alin, S. R., Cosca, C., Harasawa, S., Kozyr, A., Nojiri, Y., O'Brien, K. M., Schuster, U., Telszewski, M., Tilbrook, B., Wada, C., Akl, J., Barbero, L., Bates, N. R., Boutin, J., Bozec, Y., Cai, W.-J., Castle, R. D., Chavez, F. P., Chen, L., Chierici, M., Currie, K., de Baar, H. J. W., Evans, W., Feely, R. A., Fransson, A., Gao, Z., Hales, B., Hardman-Mountford, N. J., Hoppema, M., Huang, W.-J., Hunt, C. W., Huss, B., Ichikawa, T., Johannessen, T., Jones, E. M., Jones, S. D., Jutterström, S., Kitidis, V., Körtzinger, A., Landschützer, P., Lauvset, S. K., Lefèvre, N., Manke, A. B., Mathis, J. T., Merlivat, L., Metzl, N., Murata, A., Newberger, T., Omar, A. M., Ono, T., Park, G.-H., Paterson, K., Pierrot, D., Ríos, A. F., Sabine, C. L., Saito, S., Salisbury, J., Sarma, V. V. S. S., Schlitzer, R., Sieger, R., Skjelvan, I., Steinhoff, T., Sullivan, K. F., Sun, H., Sutton, A. J., Suzuki, T., Sweeney, C., Takahashi, T., Tjiputra, J., Tsurushima, N., van Heuven, S. M. A. C., Vandemark, D., Vlahos, P., Wallace, D. W. R., Wanninkhof, R., and Watson, A. J.: An update to the Surface Ocean CO_2 Atlas (SOCAT version 2), Earth System Science Data, 6, 69–90, https://doi.org/10.5194/essd-6-69-2014, http://www.earth-syst-sci-data.net/6/69/2014/, 2014.

Bakker, D. C. E., Pfeil, B., Landa, C. S., Metzl, N., O'Brien, K. M., Olsen, A., Smith, K., Cosca, C., Harasawa, S., Jones, S. D., Nakaoka, S.-I., Nojiri, Y., Schuster, U., Steinhoff, T., Sweeney, C., Takahashi, T., Tilbrook, B., Wada, C., Wanninkhof, R., Alin, S. R., Balestrini, C. F., Barbero, L., Bates, N. R., Bianchi, A. A., Bonou, F., Boutin, J., Bozec, Y., Burger, E. F., Cai, W.-J., Castle, R. D., Chen, L., Chierici, M., Currie, K., Evans, W., Featherstone, C., Feely, R. A., Fransson, A., Goyet, C., Greenwood, N., Gregor, L., Hankin, S., Hardman-Mountford, N. J., Harlay, J., Hauck, J., Hoppema, M., Humphreys, M. P., Hunt, C. W., Huss, B., Ibánhez, J. S. P., Johannessen, T., Keeling, R., Kitidis, V., Körtzinger, A., Kozyr, A., Krasakopoulou, E., Kuwata, A., Landschützer, P., Lauvset, S. K., Lefèvre, N., Lo Monaco, C., Manke, A., Mathis, J. T., Merlivat, L., Millero, F. J., Monteiro, P. M. S., Munro, D. R., Murata, A., Newberger, T., Omar, A. M., Ono, T., Paterson, K., Pearce, D., Pierrot, D., Robbins, L. L., Saito, S., Salisbury, J., Schlitzer, R., Schneider, B., Schweitzer, R., Sieger, R., Skjelvan, I., Sullivan, K. F., Sutherland, S. C., Sutton, A. J., Tadokoro, K., Telszewski, M., Tuma, M., van Heuven, S. M. A. C., Vandemark, D., Ward, B., Watson, A. J., and Xu, S.: A multi-decade record of high-quality fCO_2 data in version 3 of the Surface Ocean CO_2 Atlas (SOCAT), Earth System Science Data, 8, 383–413, https://doi.org/10.5194/essd-8-383-2016, http://www.earth-syst-sci-data.net/8/383/2016/, 2016.

Borges, A. V., Delille, B., and Frankignoulle, M.: Budgeting sinks and sources of CO2 in the coastal ocean: Diversity of ecosystems counts, Geophys. Res. Lett., 32, L14 601, https://doi.org/10.1029/2005GL023053, 2005.

Cai, W. J.: Estuarine and coastal ocean carbon paradox: CO2 sinks or sites of terrestrial carbon incineration?, Annu. Rev. Mar. Sci., 3, 123–145, 2011.

Cai, W.-J., Dai, M. H., and C., W. Y.: Air sea exchange of carbon dioxide in ocean margins: A province based synthesis, Geophys. Res. Lett., 33, L12 603, https://doi.org/10.1029/2006GL026219, 2006.

Chen, C. T. A. and Borges, A. V.: Reconciling opposing views on carbon cycling in the coastal ocean: continental shelves as sinks and near-shore ecosystems as sources of atmospheric CO2, Deep-Sea Res. Pt. II, 56, 578–590, 2009.

Chen, C.-T. A., Wang, S.-L., and Bychkov, A. S.: Carbonate chemistry of the Sea of Japan, Journal of Geophysical Research: Oceans, 100, 13 737–13 745, https://doi.org/10.1029/95JC00939, https://agupubs.onlinelibrary.wiley.com/doi/abs/10.1029/95JC00939, 1995.

Chen, C. T. A., Huang, T. H., Chen, Y. C., Bai, Y., He, X., and Kang, Y.: Air–sea exchanges of CO2 in the world's coastal seas, Biogeosciences, 10, 6509–6544, https://doi.org/10.5194/bg-10-6509-2013, 2013.

Dai, M., Cao, Z., Guo, X., Zhai, W., Liu, Z., Yin, Z., Xu, Y., Gan, J., Hu, J., and Du, C.: Why are some marginal seas sources of atmospheric CO2?, Geophys. Res. Lett., 40, 2154–2158, https://doi.org/10.1002/grl.50390, 2013.

de Boyer Montegut, C., Madec, G., Fischer, A. S., Lazar, A., and Iudicone, D.: Mixed layer depth over the global ocean: An examination of profile data and a profile-based climatology, Journal of Geophysical Research, 109, C12 003, https://doi.org/10.1029/2004JC002378, 2004.

Fennel, K., Wilkin, J., Previdi, M., and Najjar, R.: Denitrification effects on air-sea CO2 flux in the coastal ocean: Simulations for the northwest North Atlantic, Geophysical Research Letters, 35, https://doi.org/10.1029/2008GL036147, https://agupubs.onlinelibrary.wiley.com/doi/abs/10.1029/2008GL036147, 2008.

Fennel, K., Alin, S., Barbero, L., Evans, W., Bourgeois, T., Cooley, S., Dunne, J., Feely, R. A., Hernandez-Ayon, J. M., Hu, X., Lohrenz, S., Muller-Karger, F., Najjar, R., Robbins, L., Shadwick, E., Siedlecki, S., Steiner, N., Sutton, A., Turk, D., Vlahos, P., and Wang, Z. A.: Carbon cycling in the North American coastal ocean: a synthesis, Biogeosciences, 16, 1281–1304, https://doi.org/10.5194/bg-16-1281-2019, https://www.biogeosciences.net/16/1281/2019/, 2019.

Franco, A. C., Gruber, N., Frölicher, T. L., and Kropuenske Artman, L.: Contrasting Impact of Future CO2 Emission Scenarios on the Extent of CaCO3 Mineral Undersaturation in the Humboldt Current System, Journal of Geophysical Research: Oceans, 123, 2018–2036, https://doi.org/10.1002/2018JC013857, https://agupubs.onlinelibrary.wiley.com/doi/abs/10.1002/2018JC013857, 2018.

Friedlingstein, P., Jones, M. W., O'Sullivan, M., Andrew, R. M., Hauck, J., Peters, G. P., Peters, W., Pongratz, J., Sitch, S., Le Quéré, C., Bakker, D. C. E., Canadell, J. G., Ciais, P., Jackson, R. B., Anthoni, P., Barbero, L., Bastos, A., Bastrikov, V., Becker, M., Bopp, L., Buitenhuis, E., Chandra, N., Chevallier, F., Chini, L. P., Currie, K. I., Feely, R. A., Gehlen, M., Gilfillan, D., Gkritzalis, T., Goll, D. S., Gruber, N., Gutekunst, S., Harris, I., Haverd, V., Houghton, R. A., Hurtt, G., Ilyina, T., Jain, A. K., Joetzjer, E., Kaplan, J. O., Kato, E., Klein Goldewijk, K., Korsbakken, J. I., Landschützer, P., Lauvset, S. K., Lefèvre, N., Lenton, A., Lienert, S., Lombardozzi, D., Marland, G., McGuire, P. C., Melton, J. R., Metzl, N., Munro, D. R., Nabel, J. E. M. S., Nakaoka, S.-I., Neill, C., Omar, A. M., Ono, T., Peregon, A., Pierrot, D., Poulter, B., Rehder, G., Resplandy, L., Robertson, E., Rödenbeck, C., Séférian, R., Schwinger, J., Smith, N., Tans, P. P., Tian, H., Tilbrook, B., Tubiello, F. N., van der Werf, G. R., Wiltshire, A. J., and Zaehle, S.: Global Carbon Budget 2019, Earth System Science Data, 11, 1783–1838, https://doi.org/10.5194/essd-11-1783-2019, https://www.earth-syst-sci-data.net/11/1783/2019/, 2019.

Frischknecht, M., Münnich, M., and Gruber, N.: Remote versus local influence of ENSO on the California Current System, Journal of Geophysical Research: Oceans, 120, 1353–1374, https://doi.org/10.1002/2014JC010531, https://agupubs.onlinelibrary.wiley.com/doi/abs/10.1002/2014JC010531, 2015.

Gruber, N.: Warming up, turning sour, losing breath: ocean biogeochemistry under global change, Philosophical Transactions of the Royal Society A: Mathematical, Physical and Engineering Sciences, 369, 1980–1996, https://doi.org/10.1098/rsta.2011.0003, https://royalsocietypublishing.org/doi/abs/10.1098/rsta.2011.0003, 2011.

Gruber, N., Gloor, M., Mikaloff Fletcher, S. E., Doney, S. C., Dutkiewicz, S., Follows, M. J., Gerber, M., Jacobson, A. R., Joos, F., Lindsay, K., Menemenlis, D., Mouchet, A., Müller, S. A., Sarmiento, J. L., and Takahashi, T.: Oceanic sources, sinks, and transport of atmospheric CO_2, Global Biogeochemical Cycles, 23, GB1005, https://doi.org/10.1029/2008GB003349, 2009.

Ibanhez, J. S. P., Diverres, D., Araujo, M., and Lefevre, N.: Seasonal and interannual variability of sea-air CO2 fluxes in the tropical Atlantic affected by the Amazon River plume, Global Biogeochem. Cy., 29, 1640–1655, https://doi.org/10.1002/2015GB005110, 2015.

Jones, S. D., Le Quéré, C., Rödenbeck, C., Manning, A. C., and Olsen, A.: A statistical gap-filling method to interpolate global monthly surface ocean carbon dioxide data, J. Adv. Model. Earth Syst., https://doi.org/10.1002/2014MS000416, 2015.

Kwon, E. Y., Kim, G., Primeau, F., Moore, W. S., Cho, H.-M., DeVries, T., Sarmiento, J. L., Charette, M. A., and Cho, Y.-K.: Global estimate of submarine groundwater discharge based on an observationally constrained radium isotope model, Geophys. Res. Lett., 41, 8438–8444, 2014.

Landschützer, P., Gruber, N., Bakker, D. C. E., Schuster, U., Nakaoka, S., Payne, M. R., Sasse, T., and Zeng, J.: A neural network-based estimate of the seasonal to inter-annual variability of the Atlantic Ocean carbon sink, Biogeosciences, 10, 7793–7815, https://doi.org/10.5194/bg-10-7793-2013, 2013.

Landschützer, P., Gruber, N., Bakker, D. C. E., and Schuster, U.: Recent variability of the global ocean carbon sink, Global Biogeochemical Cycles, 28, 927–949, https://doi.org/10.1002/2014GB004853., 2014.

Landschützer, P., Gruber, N., and Bakker, D. C. E.: A 30 years observation-based global monthly gridded sea surface pCO2 product from 1982 through 2011, Carbon Dioxide Information Analysis Center, Oak Ridge National Laboratory, US Department of Energy, Oak Ridge, Tennessee, https://doi.org/10.3334/CDIAC/OTG.SPCO2_1982_2011_ETH_SOM-FFN, 2015.

Landschützer, P., Gruber, N., and Bakker, D. C. E.: Decadal variations and trends of the global ocean carbon sink, Global Biogeochemical Cycles, 30, 1396–1417, https://doi.org/10.1002/2015GB005359, http://dx.doi.org/10.1002/2015GB005359, 2016.

Landschützer, P., Laruelle, G., Roobaert, A., and Regnier, P.: A combined global ocean pCO2 climatology combining open ocean and coastal areas (NCEI Accession 0209633), NOAA National Centers for Environmental Information, https://doi.org/https://doi.org/10.25921/qb25-f418, 2020.

Laruelle, G. G., Dürr, H. H., Slomp, C. P., and Borges, A. V.: Evaluation of sinks and sources of CO2 in the global coastal ocean using a spatially-explicit typology of estuaries and continental shelves, Geophys. Res. Lett., 37, L15 607, https://doi.org/10.1029/2010gl043691, 2010.

Laruelle, G. G., Dürr, H. H., Lauerwald, R., Hartmann, J., Slomp, C. P., Goossens, N., and Regnier, P. A. G.: Global multi-scale segmentation of continental and coastal waters from the watersheds to the continental margins, Hydrol. Earth Syst. Sci., 17, 2029–2051, https://doi.org/10.5194/hess-17-2029-2013, 2013.

Laruelle, G. G., Lauerwald, R., Pfeil, B., and Regnier, P.: Regionalized global budget of the CO2 exchange at the air-water interface in continental shelf seas, Global Biogeochem. Cy., 28, 1199–1214, https://doi.org/doi.org/10.1002/2014GB004832, 2014.

Laruelle, G. G., Lauerwald, R., Rotschi, J., Raymond, P. A., Hartmann, J., and Regnier, P.: Seasonal response of air - water CO2 exchange along the land - ocean aquatic continuum of the northeast North American coast, Biogeosciences, 12, 1447–1458, https://doi.org/10.5194/bg-12-1447-2015, 2015.

Laruelle, G. G., Landschützer, P., Gruber, N., Tison, J.-L., Delille, B., and Regnier, P.: Global high-resolution monthly $p\mathrm{CO_2}$ climatology for the coastal ocean derived from neural network interpolation, Biogeosciences, 14, 4545–4561, https://doi.org/10.5194/bg-14-4545-2017, https://www.biogeosciences.net/14/4545/2017/, 2017.

Laruelle, G. G., Cai, W. J., Hu, X., Gruber, N., Mackenzie, F. T., and Regnier, P.: Continental shelves as a variable but increasing global sink for atmospheric carbon dioxide, Nature Communications, 9(1), 454, https://doi.org/10.1038/s41467-017-02738-z, 2018.

Le Quéré, C., Andrew, R. M., Friedlingstein, P., Sitch, S., Hauck, J., Pongratz, J., Pickers, P. A., Korsbakken, J. I., Peters, G. P., Canadell, J. G., Arneth, A., Arora, V. K., Barbero, L., Bastos, A., Bopp, L., Chevallier, F., Chini, L. P., Ciais, P., Doney, S. C., Gkritzalis, T., Goll, D. S., Harris, I., Haverd, V., Hoffman, F. M., Hoppema, M., Houghton, R. A., Hurtt, G., Ilyina, T., Jain, A. K., Johannessen, T., Jones, C. D., Kato, E., Keeling, R. F., Goldewijk, K. K., Landschützer, P., Lefèvre, N., Lienert, S., Liu, Z., Lombardozzi, D., Metzl, N., Munro, D. R., Nabel, J. E. M. S., Nakaoka, S.-I., Neill, C., Olsen, A., Ono, T., Patra, P., Peregon, A., Peters, W., Peylin, P., Pfeil, B., Pierrot, D., Poulter, B., Rehder, G., Resplandy, L., Robertson, E., Rocher, M., Rödenbeck, C., Schuster, U., Schwinger, J., Séférian, R., Skjelvan, I., Steinhoff, T., Sutton, A., Tans, P. P., Tian, H., Tilbrook, B., Tubiello, F. N., van der Laan-Luijkx, I. T., van der Werf, G. R., Viovy, N., Walker, A. P., Wiltshire, A. J., Wright, R., Zaehle, S., and Zheng, B.: Global Carbon Budget 2018, Earth System Science Data, 10, 2141–2194, https://doi.org/10.5194/essd-10-2141-2018, https://www.earth-syst-sci-data.net/10/2141/2018/, 2018.

Lefevre, N., Diverrés, D., and Gallois, F.: Origin of CO2 undersaturation in the western tropical Atlantic, Tellus B: Chemical and Physical Meteorology, 62, 595–607, https://doi.org/10.1111/j.1600-0889.2010.00475.x, https://doi.org/10.1111/j.1600-0889.2010.00475.x, 2010.

Lefevre, N., Caniaux, G., Janicot, S., and Gueye, A. K.: Increased CO2 outgassing in February-May 2010 in the tropical Atlantic following the 2009 Pacific El Niño, Journal of Geophysical Research: Oceans, 118, 1645–1657, https://doi.org/10.1002/jgrc.20107, https://agupubs.onlinelibrary.wiley.com/doi/abs/10.1002/jgrc.20107, 2013.

Liu, K.-K., Atkinson, L., Quinones, R., and Talaue-McManus, L., eds.: Carbon and Nutrient Fluxes in Continental Margins, Global Change - The IGBP Series, Springer Verlag, 2010.

Lovecchio, E., Gruber, N., and Münnich, M.: Mesoscale contribution to the long-range offshore transport of organic carbon from the Canary Upwelling System to the open North Atlantic, Biogeosciences, 15, 5061–5091, https://doi.org/10.5194/bg-15-5061-2018, https://www.biogeosciences.net/15/5061/2018/, 2018.

Lovely, A., Loose, B., Schlosser, P., McGillis, W., C., Z., Perovich, D., Brown, S., Morell, T., Hsueh, D., and Friedrich, R.: The Gas Transfer through Polar Sea ice experiment: Insights into the rates and pathways that determine geochemical fluxes, J. Geophys. Res.-Ocean, 120, 8177–8194, 2015.

Lynn, R. and Bograd, S.: Dynamic evolution of the 1997–1999 El Niño–La Niña cycle in the southern California Current System, Progress in Oceanography, 54, 59 – 75, https://doi.org/https://doi.org/10.1016/S0079-6611(02)00043-5, http://www.sciencedirect.com/science/article/pii/S0079661102000435, observations of the 1997-98 El Nino along the West Coast of North America, 2002.

Majkut, J. D., Sarmiento, J. L., and Rodgers, K. B.: A growing oceanic carbon uptake: Results from an inversion study of surface pCO_2 data, Global Biochemical Cycles, 28, 335–351, https://doi.org/10.1002/2013GB004585, 2014.

Mikaloff Fletcher, S. E., Gruber, N., Jacobson, A. R., Doney, S. C., Dutkiewicz, S., Gerber, M., Follows, M., Joos, F., Lindsay, K., Menemenlis, D., Mouchet, A., Müller, S. A., and Sarmiento, J. L.: Inverse estimates of anthropogenic CO_2 uptake, transport, and storage by the ocean, Global Biogeochemical Cycles, 20, GB2002, https://doi.org/10.1029/2005GB002530, 2006.

Park, G.-H., Lee, K., Tishchenko, P., Min, D.-H., Warner, M. J., Talley, L. D., Kang, D.-J., and Kim, K.-R.: Large accumulation of anthropogenic CO2 in the East (Japan) Sea and its significant impact on carbonate chemistry, Global Biogeochemical Cycles, 20, https://doi.org/10.1029/2005GB002676, https://agupubs.onlinelibrary.wiley.com/doi/abs/10.1029/2005GB002676, 2006.

Pfeil, B., Olsen, A., Bakker, D. C. E., Hankin, S., Koyuk, H., Kozyr, A., Malczyk, J., Manke, A., Metzl, N., Sabine, C. L., Akl, J., Alin, S. R., Bates, N., Bellerby, R. G. J., Borges, A., Boutin, J., Brown, P. J., Cai, W.-J., Chavez, F. P., Chen, A., Cosca, C., Fassbender, A. J., Feely, R. A., González-Dávila, M., Goyet, C., Hales, B., Hardman-Mountford, N., Heinze, C., Hood, M., Hoppema, M., Hunt, C. W., Hydes, D., Ishii, M., Johannessen, T., Jones, S. D., Key, R. M., Körtzinger, A., Landschützer, P., Lauvset, S. K., Lefèvre, N., Lenton, A., Lourantou, A., Merlivat, L., Midorikawa, T., Mintrop, L., Miyazaki, C., Murata, A., Nakadate, A., Nakano, Y., Nakaoka, S., Nojiri, Y., Omar, A. M., Padin, X. A., Park, G.-H., Paterson, K., Perez, F. F., Pierrot, D., Poisson, A., Rios, A. F., Santana-Casiano, J. M., Salisbury, J., Sarma, V. V. S. S., Schlitzer, R., Schneider, B., Schuster, U., Sieger, R., Skjelvan, I., Steinhoff, T., Suzuki, T., Takahashi, T., Tedesco, K., Telszewski, M., Thomas, H., Tilbrook, B., Tjiputra, J., Vandemark, D., Veness, T., Wanninkhof, R., Watson, A. J., Weiss, R., Wong, C. S., and Yoshikawa-Inoue, H.: A uniform, quality controlled Surface Ocean CO_2 Atlas (SOCAT), Earth System Science Data, 5, 125–143, https://doi.org/10.5194/essd-5-125-2013, 2013.

Rayner, N. A., Parker, D. E., Horton, E. B., Folland, C. K., Alexander, L. V., Rowell, D. P., Kent, E. C., and Kaplan, A.: Global analyses of sea surface temperature, sea ice, and night marine air temperature since the late nineteenth century, Journal of Geophysical Research, 108, 4407, https://doi.org/10.1029/2002JD002670, 2003.

Regnier, P., Friedlingstein, P., Ciais, P., Mackenzie, F. T., Gruber, N., Janssens, I. A., Laruelle, G. G., Lauerwald, R., Luyssaert, S., Andersson, A. J., Arndt, S., Arnosti, C., Borges, A. V., Dale, A. W., Gallego-Sala, A., Godderis, Y., Goossens, N., Hartmann, J., Heinze, C., Ilyina, T., Joos, F., LaRowe, D. E., Leifeld, J., Meysman, F. J. R., Munhoven, G., Raymond, P. A., Spahni, R., Suntharalingam, P., and Thullner, M.: Anthropogenic perturbation of the carbon fluxes from land to ocean, Nat. Geosci., 6, 597–607, https://doi.org/10.1038/ngeo1830, 2013.

Resplandy, L., Keeling, R. F., Rödenbeck, C., Stephens, B. B., Khatiwala, S., Rodgers, K. B., Long, L., M. C. B., and Tans, P. P.: Revision of global carbon fluxes based on a reassessment of oceanic and riverine carbon transport, Nature Geoscience, 11(7), 504–509, https://doi.org/Nature Geoscience, 2018.

Rödenbeck, C., Bakker, D. C. E., Metzl, N., Olsen, A., Sabine, C., Cassar, N., Reum, F., Keeling, R. F., and Heimann, M.: Interannual sea-air CO_2 flux variability from an observation-driven ocean mixed-layer scheme, Biogeosciences, 11, 4599–4613, https://doi.org/10.5194/bg-11-4599-2014, http://www.biogeosciences.net/11/4599/2014/, 2014.

Rödenbeck, C., Bakker, D., Gruber, N., Iida, Y., Jacobson, A. R., Jones, S., Landschützer, P., Metzl, N., Nakaoka, S., Olsen, A., Park, G.-H., Peylin, P., Rodgers, K. B., Sasse, T. P., Schuster, U., Shutler, J. D., Valsala, V., Wanninkhof, R., and Zeng, J.: Data-based estimates of the ocean carbon sink variability – first results of the Surface Ocean pCO2 Mapping intercomparison (SOCOM), Biogeosciences Discuss., 12, 14 049–14 104, https://doi.org/10.5194/bgd-12-14049-2015, 2015, 2015.

Roobaert, A., Laruelle, G. G., Landschützer, P., and Regnier, P.: Uncertainty in the global oceanic CO2 uptake induced by wind forcing: quantification and spatial analysis, Biogeosciences, 15, 1701–1720, https://doi.org/10.5194/bg-15-1701-2018, 2018.

Roobaert, A., Laruelle, G. G., Landschützer, P., Gruber, N., Chou, L., and Regnier, P.: The Spatiotemporal Dynamics of the Sources and Sinks of CO2 in the Global Coastal Ocean, Global Biogeochemical Cycles, 33, 1693–1714, https://doi.org/10.1029/2019GB006239, https://agupubs.onlinelibrary.wiley.com/doi/abs/10.1029/2019GB006239, 2019.

Sabine, C. L., Hankin, S., Koyuk, H., Bakker, D. C., Pfeil, B., Olsen, A., Metzl, N., Kozyr, A., Fassbender, A., Manke, A., Malczyk, J., Akl, J., Alin, S. R., Bellerby, R. G. J., Borges, A., Boutin, J., Brown, P. J., Cai, W.-J., Chavez, F. P., Chen, A., Cosca, C., Feely, R. A., González-Dávila, A., Goyet, C., Hardman-Mountford, N., Heinze, C., Hoppema, M., Hunt, C. W., Hydes, D., Ishii, M., Johannessen, T., Key, R. M., Körtzinger, A., Landschützer, P., Lauvset, S. K., Lefèvre, N., Lenton, A., Lourantou, A., Merlivat, L., Midorikawa, T., Mintrop, L., Miyazaki, C., Murata, A., Nakadate, A., Nakano, Y., Nakaoka, S., Nojiri, Y., Omar, A. M., Padin, X. A., Park, G.-H., Paterson, K., Perez, F. F., Pierrot, D., Poisson, A., Rios, A. F., Salisbury, J., Santana-Casiano, J. M., Sarma, V. V. S. S., Schlitzer, R., Schneider, B., Schuster, U., Sieger, R., Skjelvan, I., Steinhoff, T., Suzuki, T., Takahashi, T., Tedesco, K., Telszewski, M., Thomas, H., Tilbrook, B., Vandemark, D., Veness, T., Watson, A. J., Weiss, R., S., W. C., and Yoshikawa-Inoue, H.: Surface Ocean CO_2 Atlas (SOCAT) gridded data products, Earth System Science Data, 5, 145–153, https://doi.org/10.5194/essd-5-145-2013, 2013.

Sarmiento, J. M., Gloor, M., Gruber, N., Beaulieu, C., Jacobson, A. R., Mikaloff Fletcher, S. E., Pacala, S., and Rodgers, K.: Trends and regional distributions of land and ocean carbon sinks, Biogeosciences, 7, 2351–2367, https://doi.org/10.5194/bg-7-2351-2010, 2010.

Schmidtko, S., Johnson, G. C., and Lyman, J. M.: MIMOC: A global monthly isopycnal upper-ocean climatology with mixed layers, Journal of Geophysical Research: Oceans, 118, 1658–1672, https://doi.org/10.1002/jgrc.20122, https://agupubs.onlinelibrary.wiley.com/doi/abs/10.1002/jgrc.20122, 2013.

Signorini, S. R., Mannino, A., Najjar Jr., R. G., Friedrichs, M. A. M., Cai, W.-J., Salisbury, J., Wang, Z. A., Thomas, H., and Shadwick, E.: Surface ocean pCO2 seasonality and sea-air CO2 flux estimates for the North American east coast, Journal of Geophysical Research: Oceans, 118, 5439–5460, https://doi.org/10.1002/jgrc.20369, https://agupubs.onlinelibrary.wiley.com/doi/abs/10.1002/jgrc.20369, 2013.

Smith, R. L., Huyer, A., Godfrey, J. S., and Church, J. A.: The Leeuwin Current off Western Australia, 1986–1987, Journal of Physical Oceanography, 21, 323–345, https://doi.org/10.1175/1520-0485(1991)021<0323:TLCOWA>2.0.CO;2, https://doi.org/10.1175/1520-0485(1991)021<0323:TLCOWA>2.0.CO;2, 1991.

Takahashi, T., Sutherland, S., Wanninkhof, R., Sweeney, C., Feely, R., Chipman, D., Hales, B., Friederich, G., Chavez, F., Sabine, C., Watson, A., Bakker, D., Schuster, U., Metzl, N., Yoshikawa-Inoue, H., Ishii, M., Midorikawa, T., Nojiri, Y., Körtzinger, A., Steinhoff, T., Hoppema, M., Olafson, J., Arnarson, T., Tilbrook, B., Johannessen, T., Olsen, A., Bellerby, R., Wong, C., Delille, B., Bates, N., and de Baar, H.: Climatological mean and decadal change in surface ocean pCO_2, and net sea-air CO_2 flux over the global oceans, Deep-Sea Research II, 56, 554–577, 2009.

Takahashi, T., Sutherland, S. C., and Kozyr, A.: Global Ocean Surface Water Partial Pressure of CO2 Database: Measurements Performed During 1957-2017 (Version 2017)., Tech. rep., ORNL/CDIAC-160, NDP-088(V2017). (NCEI Accession 0160492). Version 4.4. NOAA National Centers for Environmental Information. Dataset.[access date 29-05-2018], https://doi.org/10.3334/CDIAC/OTG.NDP088(V2015), 2018.

Thomas, H., Bozec, Y., Elkalay, K., and De Baar, H. J. W.: Enhanced open ocean storage of CO2 from shelf sea pumping, Science, 304(5673), 1005–1008, https://doi.org/10.1126/science.1095491, 2004.

Walsh, J. J., ed.: On the nature of continental shelves, Academic Press, 1988.

Wanninkhof, R. and Trinanes, J.: The impact of changing wind speeds on gas transfer and its effect on global air-sea CO2 fluxes, Global Biogeochemical Cycles, 31, 961–974, https://doi.org/10.1002/2016GB005592, https://agupubs.onlinelibrary.wiley.com/doi/abs/10.1002/2016GB005592, 2017.

Wanninkhof, R., Park, G. H., Takahashi, T., Sweeney, C., Feely, R., Nojiri, Y., Gruber, N., Doney, S. C., McKinley, G. A., Lenton, A., Le Quéré, C., Heinze, C., Schwinger, J., Graven, H., and Khatiwala, S.: Global ocean carbon uptake: magnitude, variability and trends, Biogeosciences, 10, 1983–2000, https://doi.org/10.5194/bg-10-1983-2013, 2013.

Yasunaka, S., Murata, A., Watanabe, E., Chierici, M., Fransson, A., van Heuven, S., Hoppema, M., Ishii, M., Johannessen, T., Kosugi, N., Lauvset, S. K., Mathis, J. T., Nishino, S., Omar, A. M., Olsen, A., Sasano, D., Takahashi, T., and Wanninkhof, R.: Mapping of the air-sea CO2 flux in the Arctic Ocean and its adjacent seas: Basin-wide distribution and seasonal to interannual variability, Polar Science, 10, 323–334, 2016.

Zscheischler, J., Mahecha, M. D., Avitabile, V., Calle, L., Carvalhais, N., Ciais, P., Gans, F., Gruber, N., Hartmann, J., Herold, M., Ichii, K., Jung, M., Landschützer, P., Laruelle, G. G., Lauerwald, R., Papale, D., Peylin, P., Poulter, B., Ray, D., Regnier, P., Rödenbeck, C., Roman-Cuesta, R. M., Schwalm, C., Tramontana, G., Tyukavina, A., Valentini, R., van der Werf, G., West, T. O., Wolf, J. E., and Reichstein, M.: Reviews and syntheses: An empirical spatiotemporal description of the global surface–atmosphere carbon fluxes: opportunities and data limitations, Biogeosciences, 14, 3685–3703, https://doi.org/10.5194/bg-14-3685-2017, https://www.biogeosciences.net/14/3685/2017/, 2017.